2

NUMERICAL ERROR COMPARISONS FOR INTEGRATION OF NEAR EARTH ORBITS IN VARIOUS COORDINATE SYSTEMS

by

Oliver Albert Schwausch, B.S.

THE UNIVERSITY OF TEXAS

ENGINEERING MECHANICS RESEARCH LABORATORY

Austin, Texas

January, 1968

NUMERICAL ERROR COMPARISONS FOR INTEGRATION OF NEAR EARTH ORBITS IN VARIOUS COORDINATE SYSTEMS

Oliver Albert Schwausch

The University of Texas
Austin, Texas

January 1968

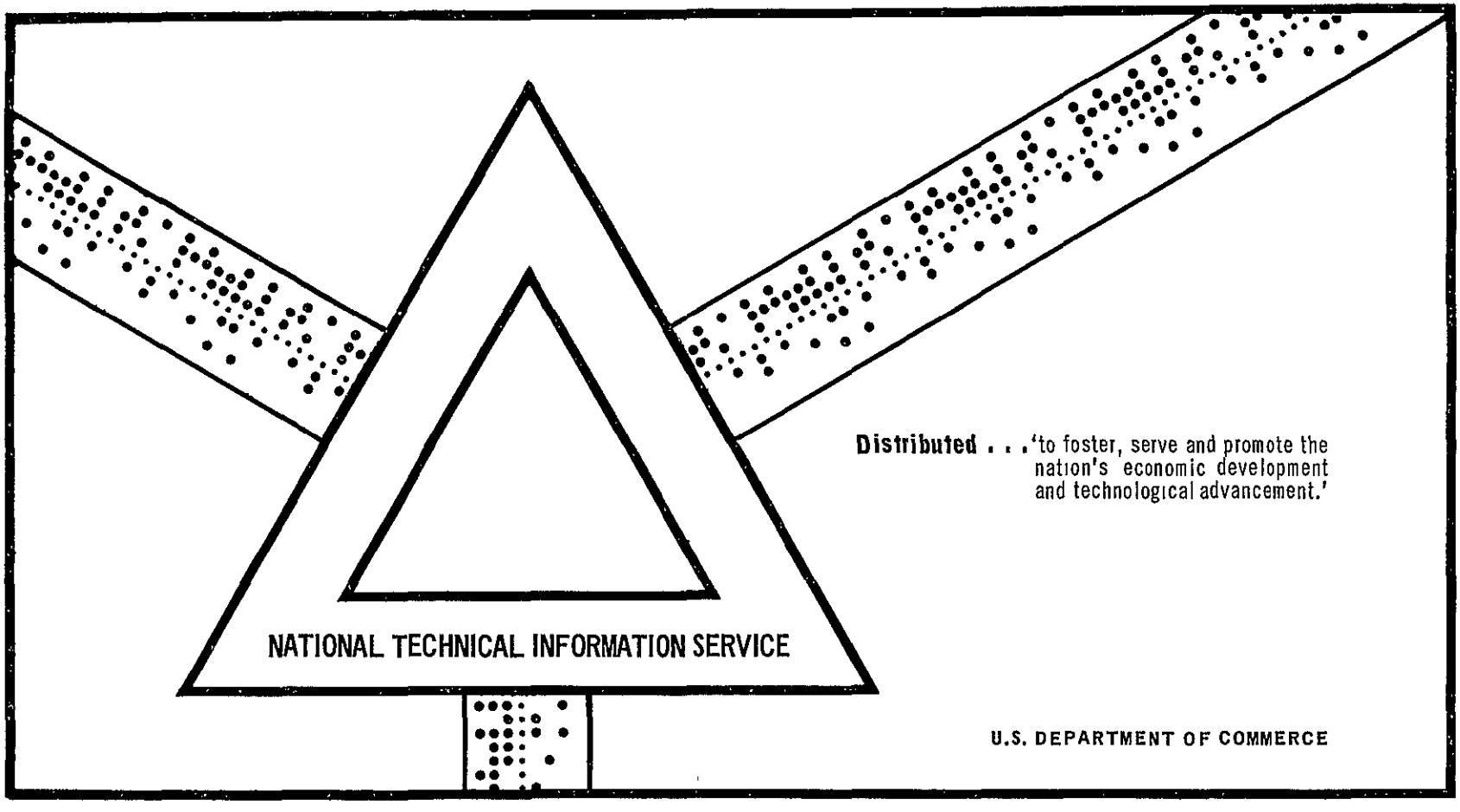

This report was prepared under

Grant NsG-551

for the

National Aeronautics and Space Administration

by the

Engineering Mechanics Research Laboratory

The University of Texas

Austin, Texas

under the direction of

Dr. Wallace T. Fowler

Assistant Professor of Aerospace Engineering

PREFACE

In order to accurately predict the state (i.e., position and velocity) of a near-Earth satellite, the equations governing the satellite's motion must be integrated numerically because the perturbations produced by atmospheric drag, an oblate Earth and celestial bodies preclude the finding of a closed form solution. Generally, the integrated states differ from the actual states, and these differences (state deviations or errors) increase with time. These state deviations are influenced to a high degree by the coordinate system in which the equations of motion are expressed. Since the two-body influence dominates the satellite's motion and since a closed form solution to the two-body problem is available, an analysis of how two-body motion is affected by different coordinate systems would provide some indication as to how the more complicated perturbed motion is affected by coordinate system choice.

The purpose of this investigation is to determine the influence which various coordinate systems have upon the error in the numerically determined value of the state for two-body motion using several integration step sizes and orbit shapes. This is accomplished by numerically integrating the equations of motion for each coordinate system under investigation. At specified time intervals an error check is made by transforming the respective position and velocity vectors to a reference coordinate system. Then a comparison of the integrated state and a reference state generated using the

solution of the two-body equation is made. In this manner the relative state errors for each system can be obtained, and the respective error norms computed. After varying the integration step size and the orbit shape, the error norms are analyzed in order to determine the sensitivity of the relative error magnitudes to step size, orbit shape and coordinate system choice.

The author wishes to express his sincere appreciation to Dr. W. T. Fowler for bringing this area of study to the author's attention, for his help and guidance throughout the course of this study and for serving as the supervising professor. The author wishes to thank Dr. B. D. Tapley and Dr. D. G. Hull for serving on the supervising committee, Dr. G. J. Lastman for his valuable suggestions and advice, Mr. Jack Hart for initial programming assistance and Mr. Jim Wiley for checking the equations of motion. Finally, the author wishes to thank his parents for their help and encouragement throughout his education and particularly his wife, Janice, for her love, patience and understanding.

The author is pleased to acknowledge the support of the National Aeronautics and Space Administration under Grant NSG-551.

Oliver A Schwausch

The University of Texas at Austin
Austin, Texas
November, 1968

TABLE OF CONTENTS

TABLE OF CONTENTS

(CONT'D)

LIST OF FIGURES

LIST OF TABLES

NOMENCLATURE

A/P	Ratio of apogee height to perigee height, where height is defined as the distance above the Earth's surface
a	Semimajor axis of satellite orbit
b	Semiminor axis of satellite orbit
C	Abbreviation for circular coordinates
d	Constant related to elliptic coordinate system
E	Eccentric anomaly
E1	Abbreviation for elliptic coordinates, set 1
E2	Abbreviation for elliptic coordinates, set 2
e	Eccentricity of satellite orbit
i	Inclination of satellite orbit to equatorial plane
ISS	Integration step size
IT	Integration time
R	Abbreviation for rectangular coordinates
R_e	Earth radius
$\bar{r}$	Position vector of satellite in orbit plane
r	Magnitude of $\bar{r}$
r_a	Apogee distance from Earth's center
r_p	Perigee distance from Earth's center
S	Abbreviation for spherical coordinates
t	Time in orbit
t_p	Time of perigee passage
(u,v,z)	Standard elliptic cylinder coordinates
(X,Y,Z)	Inertial geocentric satellite coordinates

NOMENCLATURE

(CONT'D)

(x,y,z)	Satellite coordinates in orbit plane (z-0)
$(\alpha_1,\alpha_2,\alpha_3)$	Nonstandard set of elliptic cylinder coordinates designated as set 1
$(\beta_1,\beta_2,\beta_3)$	Nonstandard set of elliptic cylinder coordinates designated as set 2
$(\gamma_1,\gamma_2,\gamma_3)$	Standard set of elliptic cylinder coordinates designated as set 3
(ρ,σ,τ)	Standard spherical coordinates
$(\rho,\cos\sigma,\cos\tau)$	Nonstandard spherical coordinates
(r,θ,z)	Standard circular cylinder coordinates
$(r,\cos\theta,z)$	Nonstandard circular cylinder coordinates
μ	Earth's gravitational constant
ϕ	True anomaly
ω	Argument of perigee
Ω	Longitude of ascending more of satellite orbit
$\bar{(\ )}$	Denotes ( ) is a vector
$\dot{(\ )}$	First derivation of ( ) with respect to time

CHAPTER I

INTRODUCTION

I.1 Purpose of Investigation

Since the launching of the first artificial Earth satellite in 1957, man has been concerned with the problems encountered in the computation of such satellite orbits. In general, this is a very difficult task to perform accurately over long time intervals. This task is usually carried out numerically because closed form solutions do not exist to the complete ordinary second-order nonlinear differential equations which govern the satellite's motion. In order to describe this motion as accurately as possible, the equations of motion must include terms accounting for all forces influencing the satellite's motion. However, since a majority of the orbiting vehicles are nonthrusting, their mass is much less than that of the Earth, and their orbits are such that the effects of the perturbing force effects are small, a fairly accurate orbit description can be obtained from two-body considerations. By assuming an inverse square force field, the two-body equation of motion can be expressed as

$$\frac{d^2\bar{r}}{dt^2} = \frac{-\mu\bar{r}}{r^3} \tag{1}$$

where μ is the Earth's gravitational constant, $\bar{r}$ is the position vector measured from the center of the Earth and r is the magnitude of the position vector. A closed form solution to Equation (1) is

given by

$$r = \frac{a(1-e^2)}{1 + e \cos \phi} \tag{2}$$

where a is the semimajor axis, e is the eccentricity and ϕ is the true anomaly (see Figure 1). Equation (2) is the equation of a conic section in polar form and consequently represents a circle ($e = 0$), an ellipse ($0 < e < 1$), a parabola ($e = 1$) or a hyperbola ($e > 1$). Since closed orbits ($e < 1$) are of the most interest, only the orbit geometry associated with $e < 1$ is shown in Figure 1. Also shown in Figure 1 is the eccentric anomaly, E, which related the elliptic motion to the equivalent circular motion. The eccentric anomaly is related to the true anomaly, ϕ, by

$$\tan E = \frac{(1-e^2)^{\frac{1}{2}} \sin \phi}{1 + e \cos \phi} \tag{3}$$

The eccentric anomaly is related to the time in orbit, t, from perigee passage, t_p, by

$$t - t_p = \left(\frac{a^3}{\mu}\right)^{\frac{1}{2}} (E - e \sin E) \tag{4}$$

Whenever the states for a two-body orbit are obtained by integrating the equations of motion numerically, the states obtained differ from those obtained via the two-body solution. The error which accumulate in the integrated states is a function of the type of orbit being integrated, the coordinate system in which the equations of motion are formulated and the size of the integration time

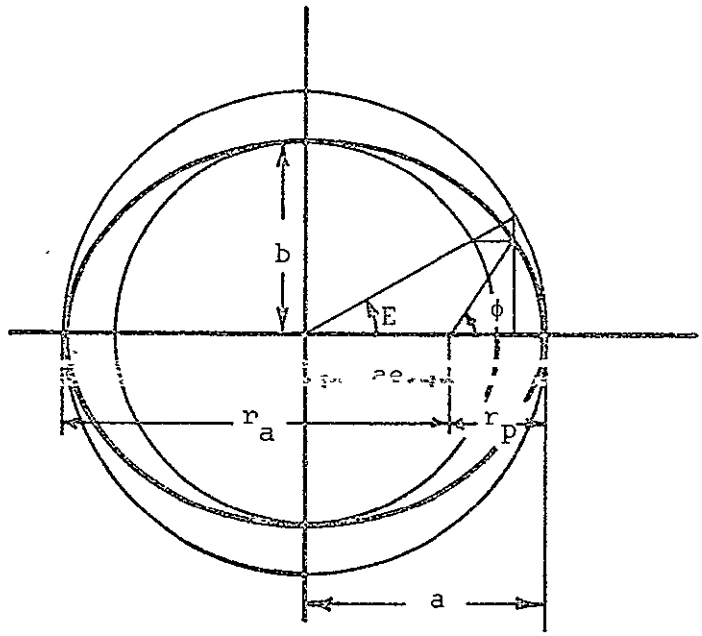

Figure 1. Elliptic Orbit Geometry

step. The manner in which the above three parameters are combined affects both the accuracy and the computational time (which can be exceedingly long in some cases such as orbital lifetime and ephermeris predictions). Because of the expense involved in computer operation, considerable emphasis is placed on efficient programming in order to reduce running time, thus conserving cost, while still achieving the greatest accuracy possible.

The purpose of this study is to investigate the relative error propagation in the state variables resulting from the numerical integration of near-Earth two-body orbits. The influence of coordinate system, integration step size, and orbit shape on the computational efficiency is examined with the emphasis being placed on accuracy and reduced running times.

I.2 Previous Studies

A previous study has been conducted by Gerber and Lewallen[1*] in which the generation of relative state error magnitudes as a function of orbit shape and integration step size for rectangular and spherical coordinate systems was investigated.

This study first determined the effects of integration step size on circular orbits. The step sizes considered ranged from 15 seconds to 120 seconds. From these results a step size of 30 seconds was selected for use in studying eccentricity variations which ranged

---

* Numbers appearing in the text as superscripts indicate references listed in the Bibliography.

for 0 to 0.3. The orbits were integrated over an interval of only 60,000 seconds because of computer core storage limitations. The computer used in this study was a Univac 1108 with a 36-bit word length. This study was carried out in single-precision arithmetic with partial double precision in the integrator only. Other assumptions and simplifications were essentially the same as the ones which will be used in the present investigation and will be discussed later.

The preliminary conclusions reached by Gerber and Lewallen were as follows. First, the velocity error norms and the position error norms exhibited the same types of behavior for both step size and eccentricity variations. Second, the errors in the spherical coordinate system were well behaved and increased linearly with accumulated integration time while the errors in the rectangular coordinate system exhibited a fairly constant amplitude periodic variation superimposed on an exponential type increase. The rectangular coordinate errors were generally larger than the spherical coordinate errors and the differences increased as the orbital eccentricity increased. Typical terminal time results are given in Table 1 where the quantity A/P refers to the ratio of apogee height to perigee height with height being defined as the distance above the Earth's surface and the quantity ISS refers to the integration step size. Third, the results indicated that a "best" numerical integration step size (a compromise between round-off and truncation errors) could exist for each coordinate system. The "best" step size

TYPICAL RESULTS - GERBER AND LEWALLEN		
Error in Position at 60,000 Seconds (feet)		
Coordinate System	A/P = 1	A/P = 2
Rectangular	1250	960
Spherical	140	265
Problem Parameters		
ISS = 30 seconds		Ω = 0.1 radian
i = 0.5 radian		ω = 0.1 radian

TABLE 1

appeared to be larger for the spherical coordinates than for rectangular coordinates. Finally, it became apparent that the errors in the state were computer word length dependent, thereby suggesting that a comparison of results obtained using full double precision and/or other computers be made.

Later unpublished work by Rainbolt and Lewallen[2] included analysis of the circular cylinder, parabolic cylinder, paraboloidal and elliptic cylinder coordinates as well as the rectangular and spherical coordinates. The elliptic cylinder coordinates used were not rectified to the orbit plane (i.e., did not take advantage of the particular form and properties of the coordinate system). This work was conducted on the Univac 1108 computer using full double-precision arithmetic. Preliminary results obtained from the investigators indicated that the parabolic cylinder coordinates exhibited smaller error generation tendencies than any of the other coordinate systems studied. Typical terminal time results for this investigation are given in Table 2.

I.3 Scope of Investigation

In the present study, five coordinate systems (rectangular, spherical, circular cylinder, and two forms of elliptic cylinder coordinates) are compared in order to determine their efficiency for numerical integration of orbital equations. These five coordinate systems were chosen from numerous coordinate systems considered in a preliminary screening process. Various combinations of eccentricity and step size are investigated in order to determine the sensitivities

TYPICAL RESULTS - RAINBOLT AND LEWALLEN		
Error in Position at 90,000 Seconds (feet)		
Coordinate System	A/P = 1	A/P = 2
Rectangular	22.4	11.0
Spherical	21.8	20.5
Paraboloidal	17.0	14.5
Elliptic Cylinder	17.5	12.5
Circular Cylinder	13.0	8.0
Parabolic Cylinder	5.8	8.0
Problem Parameters		
ISS = 15 seconds	Ω = 1.0 radian	
i = 0.5 radian	ω = 1.0 radian	

TABLE 2

of the coordinate systems studied to orbit shape and integration step size. The eccentricities range from 0 to 0.2 while the integration step sizes range from 15 seconds to 120 seconds.

CHAPTER II

ANALYSIS

II.1 Simplifying Assumptions

The assumptions made concerning the orbits treated in this study are as follows. The types of orbits considered are high enough so that the atmospheric drag can be neglected but low enough so that the celestial body perturbations can also be neglected. The orbiting satellite is nonthrusting and it is assumed that the Earth can be represented by a spherical body of homogeneous mass distribution.

II.2 Selection of Variables and Constants

In order to assure that realistic orbit shapes and integration step sizes are used in this investigation, care must be taken in selecting the values of these parameters. The orbits chosen should be representative of two-body motion, and the time stpes should be realistic ones.

The motion of a body moving in a two-body orbit can be defined by specifying six quantities (orbital elements). The standard orbital elements are the semimajor axis, a, the orbital eccentricity, e, the orbit inclination, i, the longitude of the ascending node, Ω, the argument of perigee, ω, and the time of perigee passage, t_p.

The function of the first two elements, a and e, is to

define the orbit's shape. For this study a and e are obtained by specifying apogee and perigee for the orbit under consideration (see Table 3).

The next three elements, i, Ω, and ω locate the orbit with respect to the inertial reference coordinate system and remain constant throughout the course of this study. These variables have been arbitrarily assigned the following values: i = 0.5 radian, Ω = 0.1 radian and ω = 0.1 radian. The remaining element, t_p, is set equal to zero since this element has no special significance for the present study as it is just a time reference.

Remaining to be specified is the integration step size, ISS. The values considered for this parameter are 15 seconds, 30 seconds, 60 seconds and 120 seconds. These values are used for all orbits studied. The relationship between integration step size and the associated error checks is given in Table 4.

Other quantities which must be specified also are the total integration time, IT, the Earth's gravitational constant, μ, and the Earth's radius, R_e. These values along with the constant orbital elements are given in Table 5.

II.3 Selection of Coordinate Systems

Prior to selecting a set of coordinate systems for detailed analysis, numerous coordinate systems were considered. Among those considered were rectangular coordinates, two forms of spherical coordinates, two forms of circular cylinder coordinates, (henceforth

VARIABLES				
Perigee Ht. (miles)	Apogee Ht. (miles)	A/P	Eccentricity	Semimajor Axis (feet)
100	100	1	0.0	2.145E+7
100	200	2	0.0125	2.172E+7
100	500	5	0.0469	2.251E+7
100	1000	10	0.0997	2.383E+7
100	2000	20	0.1895	2.649E+7
ISS = 15, 30, 60, 120 seconds				

TABLE 3

STEP SIZE - ERROR CHECK RELATIONS				
Step Size (seconds)	Number of Integration Steps	Number of Error Checks	Steps Between Checks	Time Between Checks (seconds)
15	12000	300	40	600
30	6000	300	20	600
60	3000	300	10	600
120	1500	300	5	600
Integration Time = 180000 seconds				

TABLE 4

CONSTANTS
$i = 0.5$ radian
$\Omega = 0.1$ radian
$\omega = 0.1$ radian
$t_p = 0.0$ seconds
$\mu = 1.407653 \times 10^{16}$ ft^3/sec^2
$R_e = 3963.115$ miles
$T = 180,000$ seconds

TABLE 5

called circular coordinates), three forms of elliptic cylinder coordinates, (henceforth called elliptic coordinates), ellipsoidal coordinates, and conical coordinates.

In the following paragraphs each coordinate system will be briefly discussed, and the reasons for either rejecting or retaining the system will be given. In an effort to increase computational efficiency, any substitution or coordinate system orientation which significantly simplifies either the coordinate transformations or the equations of motion is employed.

II.3.1 Reference Coordinate System

The coordinate system chosen as a reference system in this study is an inertial Earth-centered rectangular coordinate system with the XY plane lying in the equatorial plane. This coordinate system, shown in Figure 2, is labeled the (X,Y,Z) system.

II.3.2 Rectangular Coordinates

This coordinate system, also designated by (X,Y,Z), is in common use and is therefore retained for the purposes of this study. The rectangular Cartesian system used coincides with the inertial reference coordinate system (See Figure 2).

II.3.3 Spherical Coordinates

Two forms of spherical coordinates (Figure 3) were considered. They were the standard spherical coordinates (ρ,σ,τ)

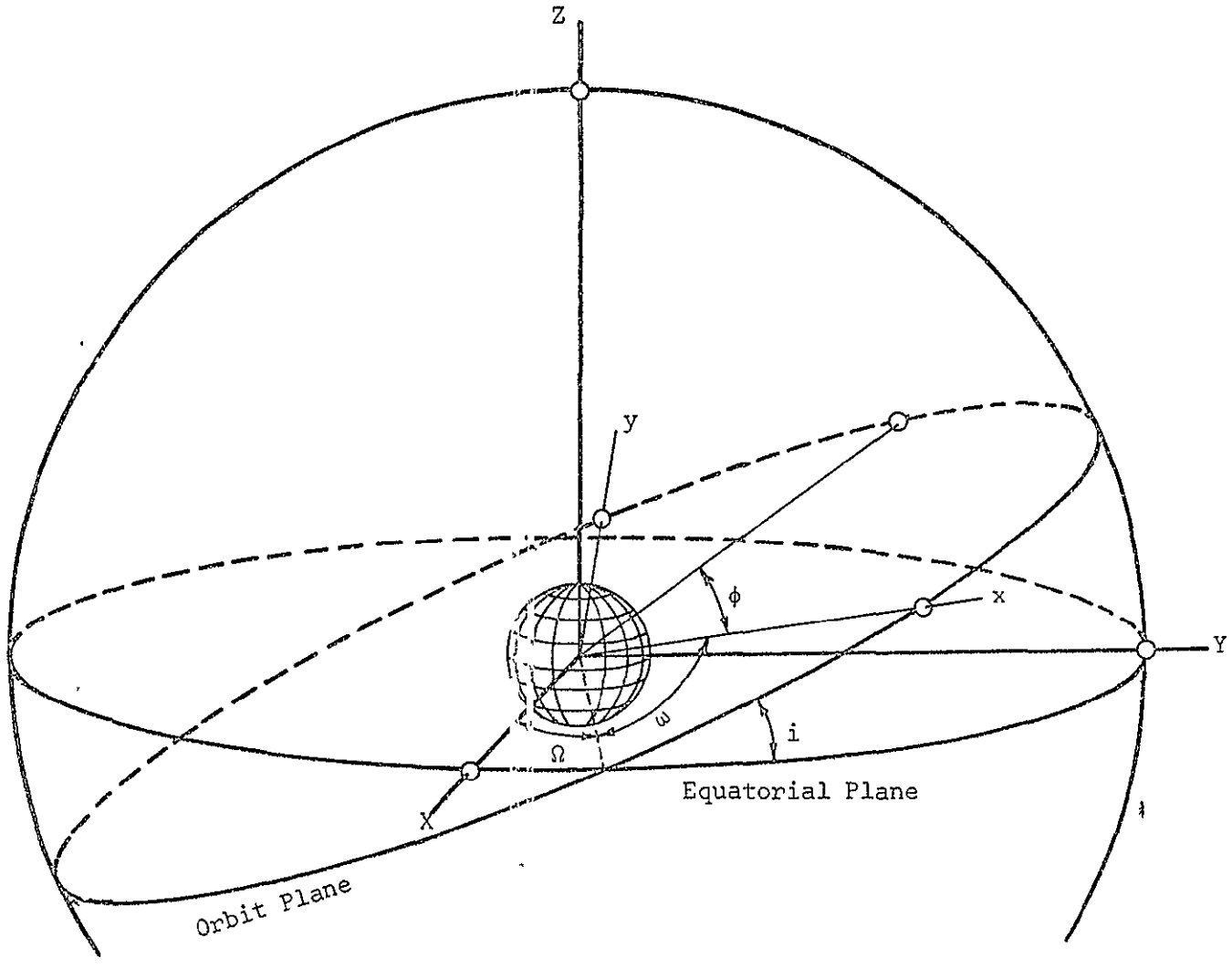

Figure 2. Reference System Geometry

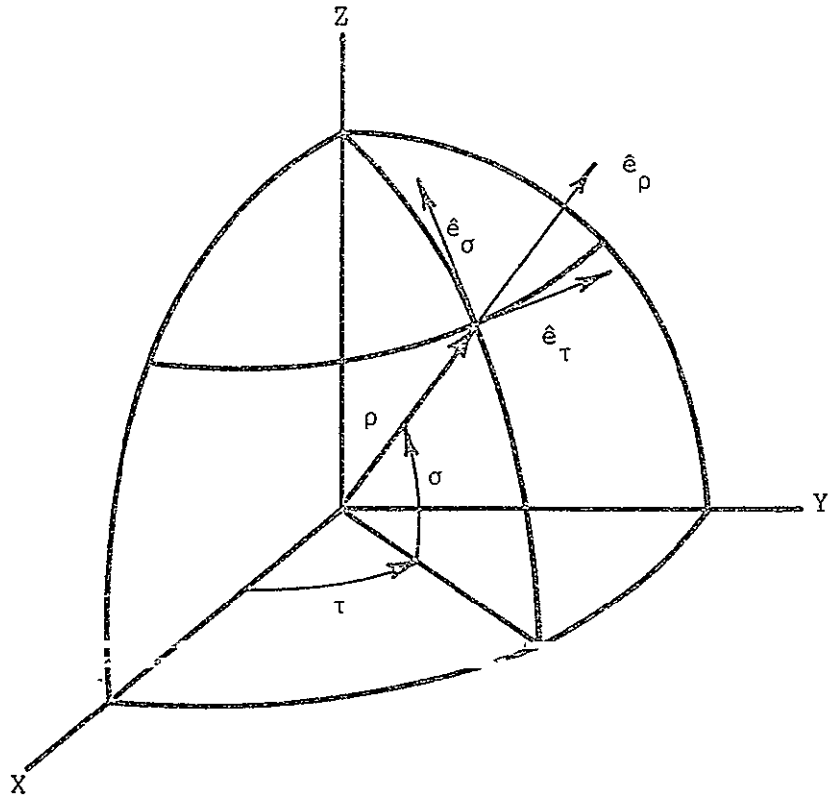

Figure 3. Spherical Coordinate System

and a nonstandard set of coordinates (ρ,cos σ,cos τ). Although the equations of motion for the nonstandard system were simple, an ambiguity in the sign of the sine term exists. In order to resolve this sign ambiguity, a sign convention employing a series of checks on the coordinate values was developed. A preliminary computational check indicated that integration of the system containing the angles was inherently more accurate than integration of the system containing the cosines of the angles. Due to the accuracy difference (probably due to the oscillatory nature of the cosine) the nonstandard system was discarded while the standard set was retained. Again, in order to eliminate a coordinate transformation, the spherical coordinate axes (X,Y,Z) of Figure 3 were aligned with (X,Y,Z) axes of the reference coordinate system.

II.3.4 Circular Coordinates

Two forms of the circular coordinates were considered (Figure 4). They were the standard set r, θ, z and a nonstandard set (r,cos θ,z). The nonstandard set exhibited accuracy problems equivalent to those of the nonstandard spherical coordinates and was rejected. The standard circular coordinates were retained and as in the previous cases, the coordinate axes (X,Y,Z) shown in Figure 4 were aligned with (X,Y,Z) axes of the reference system.

II.3.5 Elliptic Coordinates

Three sets of elliptic coordinates (Figure 5) were considered. Set 1 designated by (α_1,α_2,α_3) and set 2 designated by

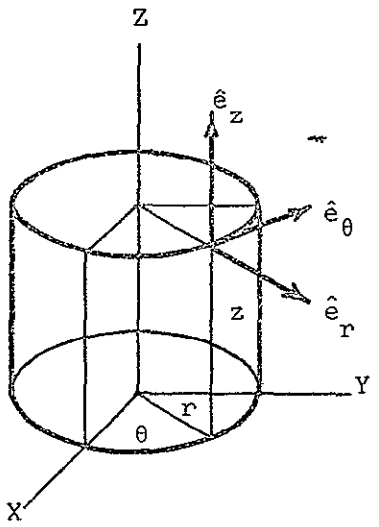

Figure 4. Circular Cylinder Coordinate System

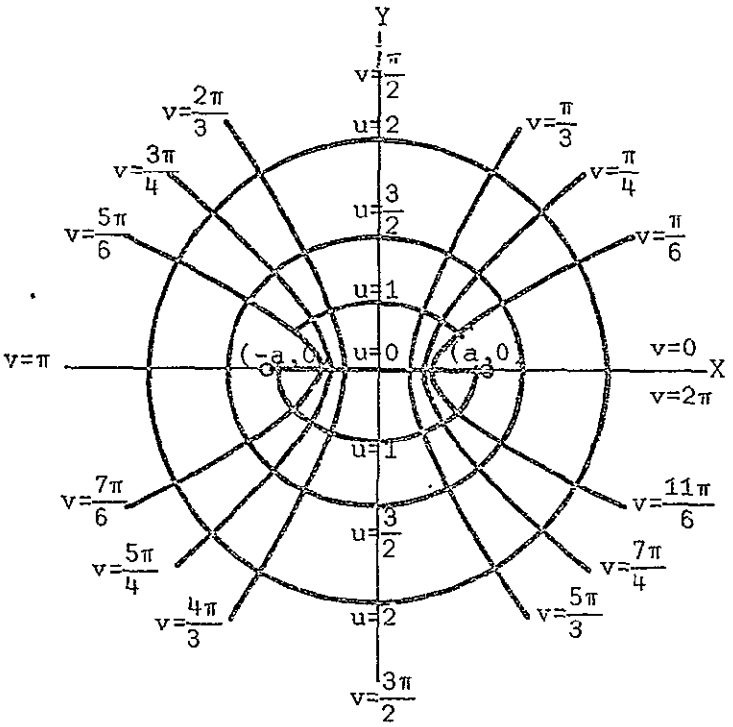

Figure 5. Elliptic Cylinder Coordinate System

$(\beta_1,\beta_2,\beta_3)$ were rectified to the orbit plane while set 3 designated by $(\gamma_1,\gamma_2,\gamma_3)$ was referenced to the inertial reference system. The coordinates of set 1 are defined by

$$\alpha_1 = d \cosh u \quad \alpha_2 = v \quad \alpha_3 = z \tag{5}$$

where d is a constant related to the coordinate geometry. The coordinates of set 1 are measured in the orbital plane. Thus, the elliptic axes (X,Y,Z) shown in Figure 5 were aligned with the x,y,z axes of Figure 2. The coordinates of set 2, also measured in the orbit plane, are defined by

$$\beta_1 = d \cosh u \quad \beta_2 = \cos v \quad \beta_3 = z \tag{6}$$

The coordinates of set 3 are defined by

$$\gamma_1 = u \quad \gamma_2 = v \quad \gamma_3 = z \tag{7}$$

where (u,v,z) are the standard elliptic coordinates shown in Figure 5 and are measured in the equatorial (XY) plane. Thus, the (X,Y,Z) axes for this set are aligned with the (X,Y,Z) axes of Figure 2. Note that in order to obtain the (X,Y,Z) (reference system) components of coordinate sets 1 and 2, the (x,y,z) components in the orbital plane (see Figure 2) must first be obtained from the respective elliptic coordinates and then transformed to the reference coordinate system using the transformations given in Appendix A.5.

The standard procedure for determining the initial values of the elliptic coordinates is to solve Equation (8) for the particular values

$$X = d \cosh u \cos u \qquad Y = d \sinh u \sin v \qquad Z = 3 \tag{8}$$

where u, v and z are the elliptic coordinates as they are ordinarily defined (set 3) and d is a constant related to the coordinate geometry (see Figure 5). Although the above transformations are straightforward, the inverse transformations (necessary in set 3) are quite complicated. However, it will be shown in the following paragraphs that a simplification of the inverse transformations is possible in orbital analysis by associating the elliptic coordinates with the orbital elements.

Consider the equation of an ellipse in the form

$$\frac{X^2}{d^2 \cosh^2 u} + \frac{Y^2}{d^2 \sinh^2 u} = 1 \tag{9}$$

Equation (9) is often used in the derivation of Equations (8).[4] The standard equation of an ellipse is given by

$$\frac{X^2}{a^2} + \frac{Y^2}{b^2} = 1 \tag{10}$$

where a is the semimajor axis and b is the semiminor axis. By comparing Equations (9) and (10), it is evident that

$$a = d \cosh u \tag{11}$$

$$b = d \sinh u \tag{12}$$

Consider now the expression for the eccentricity in the form

$$e = \left[\frac{a^2 - b^2}{a^2}\right]^{\frac{1}{2}} \tag{13}$$

Substituting Equations (11) and (12) into Equation (13) yields

$$e = \left[\frac{d^2 \cosh^2 u - d^2 \sinh^2 u}{d^2 \cosh^2 u}\right]^{\frac{1}{2}} \tag{14}$$

which reduces to

$$e = \left[\frac{1}{\cosh^2 u}\right]^{\frac{1}{2}} \tag{15}$$

or

$$\cosh u = \frac{1}{e} \tag{16}$$

Substituting Equation (16) into Equation (11) yields

$$d = ae \tag{17}$$

Note that if u is chosen as one of the coordinates, then from Equation (16) u is given by

$$u = \cosh^{-1}\left(\frac{1}{e}\right) \tag{18}$$

which is singular for circular orbits (zero eccentricity). However,

by defining the coordinate as $d \cosh u$, this singularity is eliminated since $d \cosh u = a$ as shown in Equation (11).

Now, recall that the parametric equations of an elliptic orbit are given by

$$x = a \cos E \qquad y = b \sin E \tag{19}$$

Solving Equations (11) and (12) for d and then substituting these equations into the respective terms of Equation (8) yields

$$X_e = a \cos v \qquad Y_e = b \sin v \tag{20}$$

A comparison of Equations (19) and (20) demands that

$$v = E \tag{21}$$

Thus, since $d \cosh u = a$ and $v = E$, coordinate sets 1 and 2 may be given by

$$\alpha_1 = a \qquad \alpha_2 = E \qquad \alpha_3 = z \tag{22}$$

and

$$\beta_1 = a \qquad \beta_2 = \cos E \qquad \beta_3 = z \tag{23}$$

Note that the coordinates as given in Equations (22) and (23) require that the xy and uv planes coincide with the orbit plane. Thus, since α_3 and β_3 are initially zero and since the motion

is constrained to the orbit plane, $\dot{\alpha}_3, \ddot{\alpha}_3, \dot{\beta}_3, \ddot{\beta}_3$ must then all necessarily be zero. In addition, since α_1 and β_1 are determined from the semimajor axis which is constant for unperturbed orbits, the terms $\dot{\alpha}_1, \ddot{\alpha}_1, \dot{\beta}_1, \ddot{\beta}_1$ are also zero. As a result of these simplifications, the only coordinates with nonzero accelerations are α_2 and β_2. If the time derivatives of these two coordinates are expressed in terms of the eccentric anomaly, the accelerations for these coordinates may be given by

$$\ddot{\alpha}_2 = \frac{-\mu e \sin E}{a^3(1 - e \cos E)^3} \tag{24}$$

and

$$\ddot{\beta}_2 = \frac{\mu(\zeta \cos E)}{a^3(1 - e \cos E)^3} \tag{25}$$

Thus, the number of coordinates to be integrated has been reduced from three to one.

Since the elliptic coordinates are referenced to the center of the ellipse (Figure 5) and since elliptic orbit motion is referenced to the focus of the ellipse (Figure 1), the origin of the elliptic coordinate system must be transferred to the focus. This is accomplished by translating the x-axis according to

$$x = \alpha_1 \cos \alpha_2 - ae \tag{26}$$

or

$$x = \beta_1\beta_2 - ae \tag{27}$$

Note that since coordinate set 3 is referenced to the equatorial plane, the simplifications as given in Equations (11) and (12) are not applicapable to these coordinates. This requires the coordinates to be determined by solving Equation (8), which is quite cumbersome. Furthermore, when referenced to the equatorial plane, all three coordinates must be integrated instead of one as in sets 1 and 2. For these reasons coordinate set 3 is discarded in this study.

II.3.6 Ellipsoidal and Conical Coordinates

The ellipsoidal and conical coordinates were discarded because of sign ambiguities arising in the coordinate transformations. The transformations from the rectangular Cartesian to the ellipsoidal and conical coordinates were also quite cumbersome.

II.4 Equations of Motion

The two-body equations of motion for the coordinate systems investigated in this study are presented in Appendix B. The equations of motion for the rectangular and the spherical coordinates were obtained from Reference 1. The equations of motion for circular and elliptic coordinates were obtained using Lagrange's equation.

II.5 Computational Procedure

The computer programs used in this study were written in

Fortran IV for the CDC 6600 computer (listings of the program are available upon request). Since this computer has a 60-bit word length and since single and double precision Univac 1108 results were available as checks, it was felt that double-precision arithmetic would be unnecessary. In order to verify this assumption some of the work was carried out in both single and double precision. No appreciable difference in accuracy was found. However, the double precision results did require a longer computational time as would be expected. The computational algorithm as used in this investigation is as follows:

1. Prior to any major calculation the transformation from the orbital plane to the reference coordinate system is generated.

2. The initial reference state in the orbit plane and the transformation to the reference coordinate system are then generated.

3. The initial conditions for each coordinate system are then set up using the necessary states formed in step two.

4. The equations of motion for each set of coordinates for the specified integration period are integrated numerically. At specified intervals the appropriate error checks are performed. The numerical integration routine (which was obtained from Fowler and Lastman - Reference 3) uses a fourth order Runge-Kutta as a starter and then shifts to a fifth order Adams predictor-corrector. As used in this investigation, the entire integration procedure was carried out in single precision.

CHAPTER III

RESULTS AND DISCUSSION

The results of this investigation are presented in the forms of graphs (Figures 6 through 19) and tables (Tables 6 through 11) showing the error in position and velocity as a function of orbit time for various combinations of step size and orbit shape. Since the errors in state range over several orders of magnitude, each coordinate error curve is scaled (if necessary) so that all the coordinate error curves for one step size and orbit shape combination can be presented on one graph. If scaling is necessary, the respective scale factor is indicated on each graph in paranthesis. Unless otherwise noted, all scale factors are one. In order to obtain the correct error values for the scaled system, simply divide the ordinate value by the indicated scale factor. An example of the raw computer plot output is shown in Figures 6 and 13 with Figure 6 showing the position error and Figure 13 the velocity error. The large oscillations of the coordinate error curves cause the curves to overlap. Therefore they do not emphasize the item of primary concern; i.e., the size of the maximum error in the vicinity of a given point in time. This is most easily shown by plotting maximum error envelopes for the various error curves. The envelopes of the curves shown in Figures 6 and 13 are shown in Figures 7 and 14. Since the graphs showing the maximum error curve envelopes are interpreted more easily than plots showing the raw

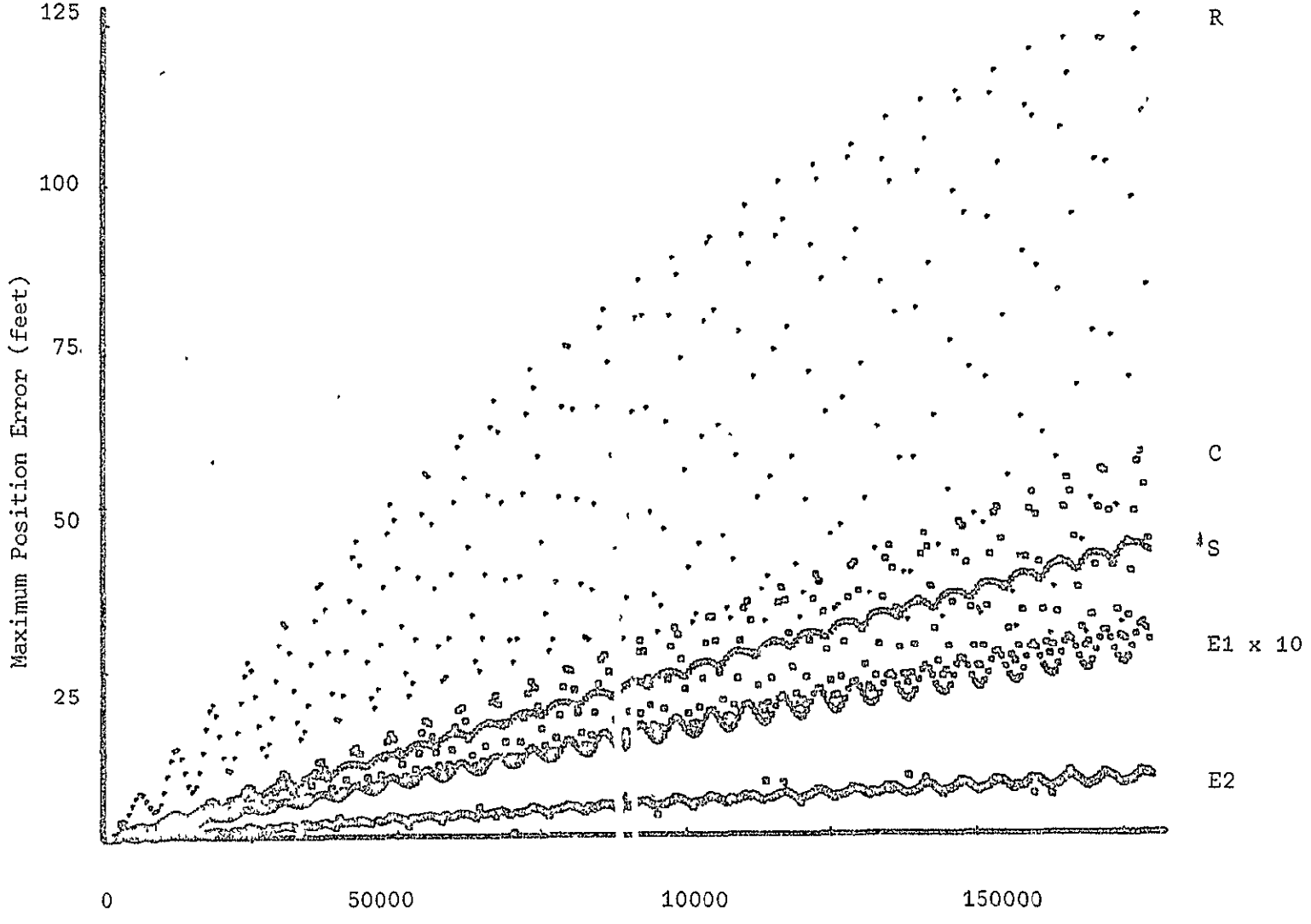

Figure 6. Raw Position Error, N = 10, ISS = 15

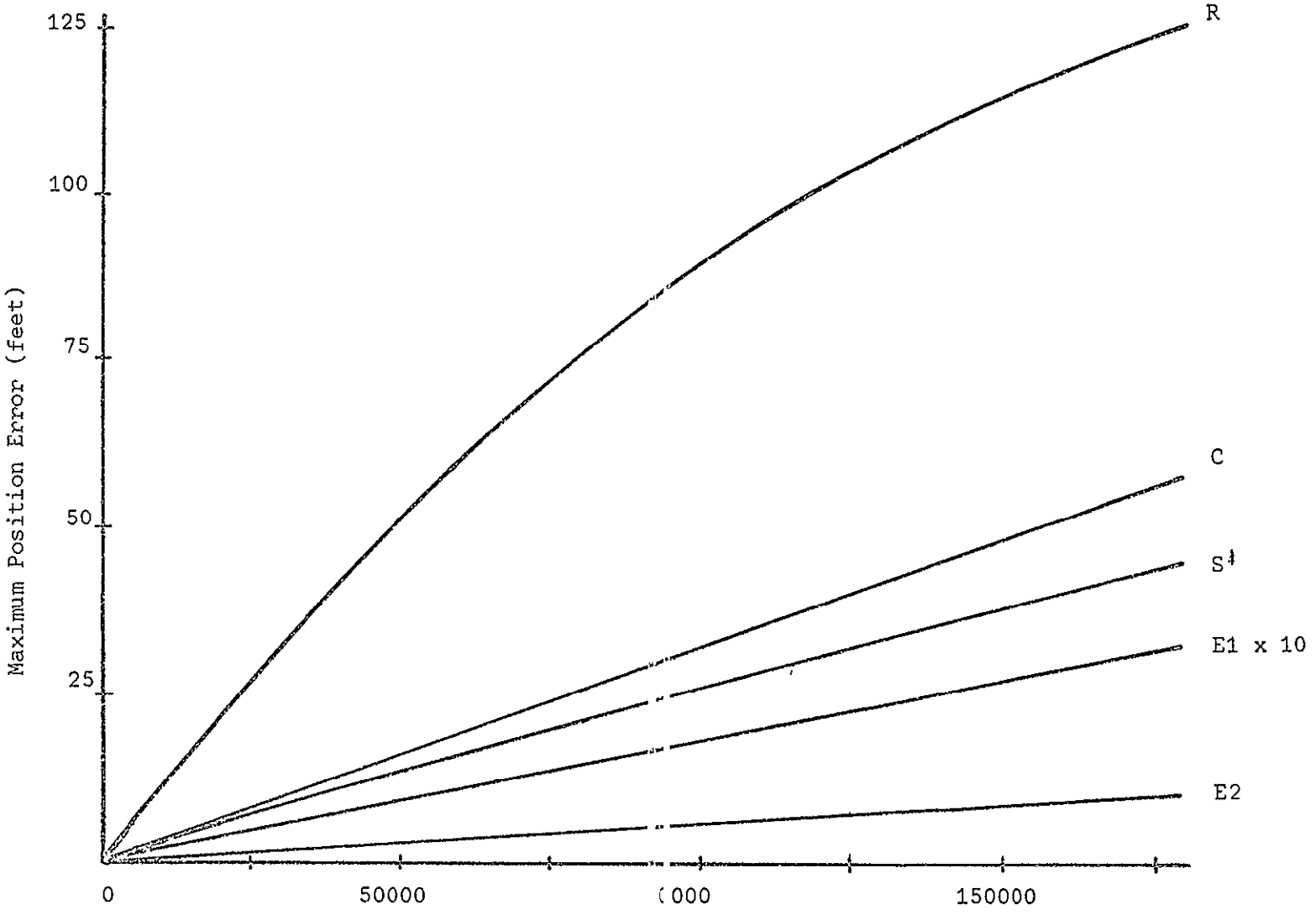

Figure 7. Maximum Position Error, .../P = 10, ISS = 15

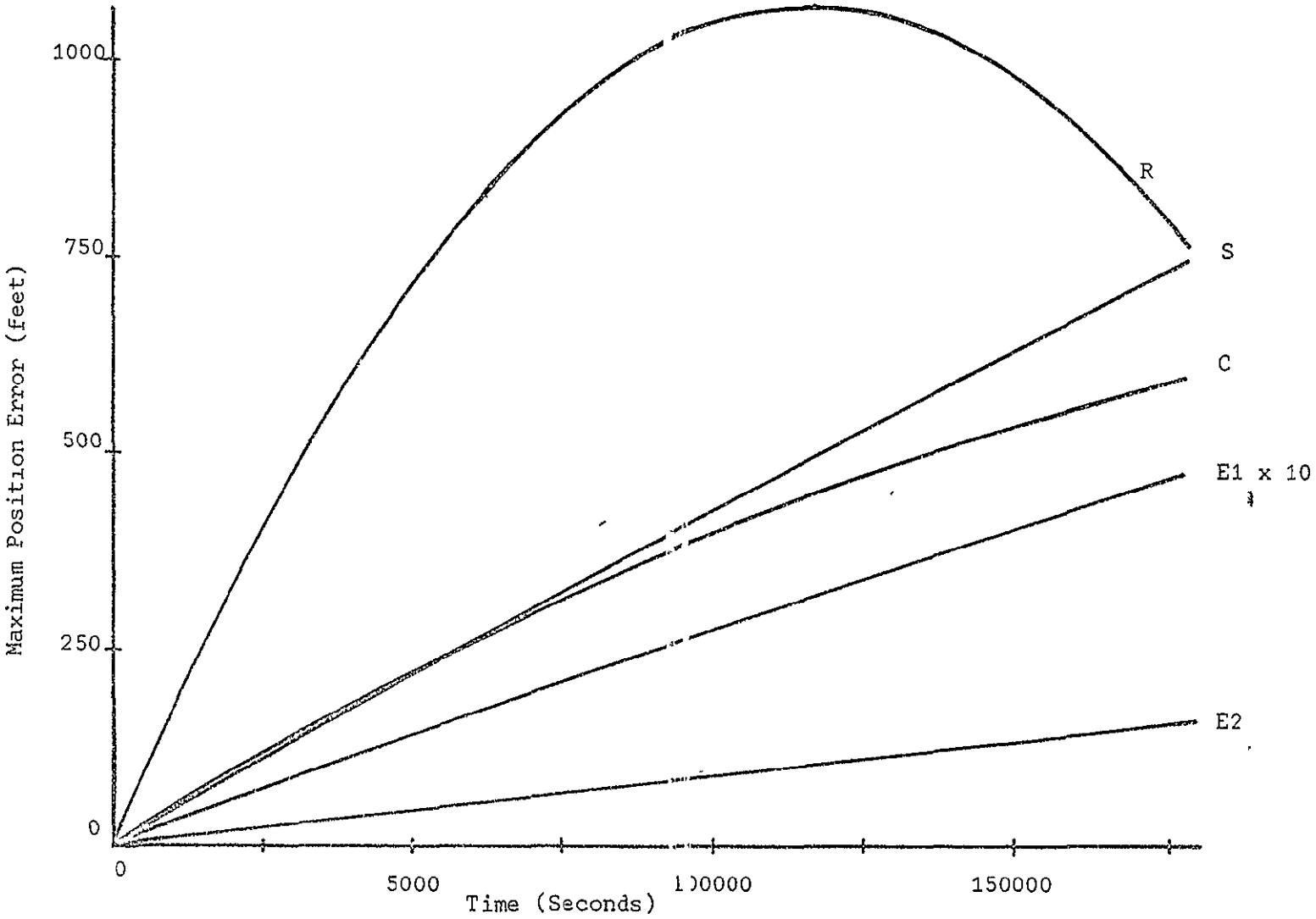

Figure 8. Maximum Position Error, NP = 10, ISS = 30

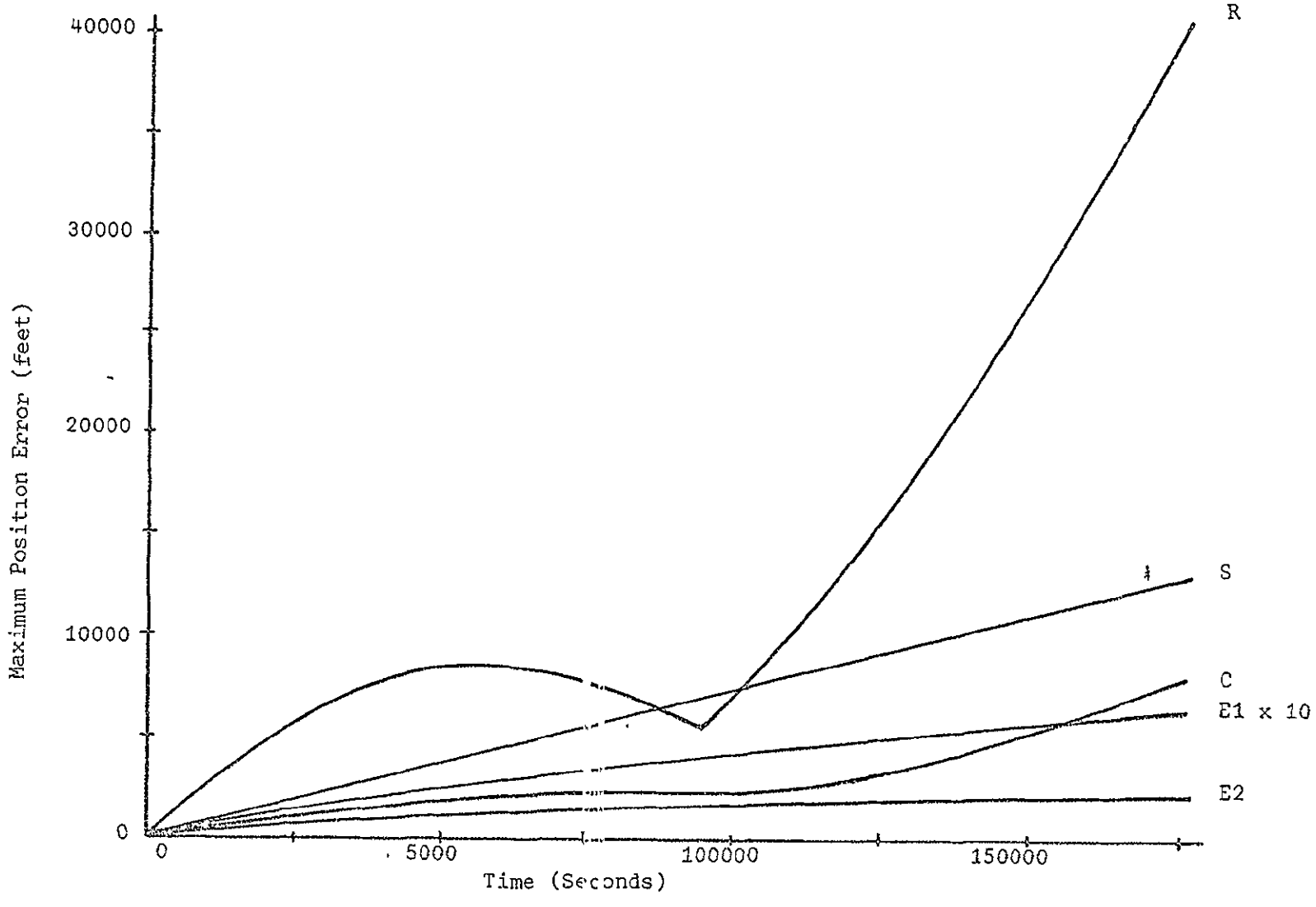

Figure 9. Maximum Position Error. A/P = 10, ISS = 60

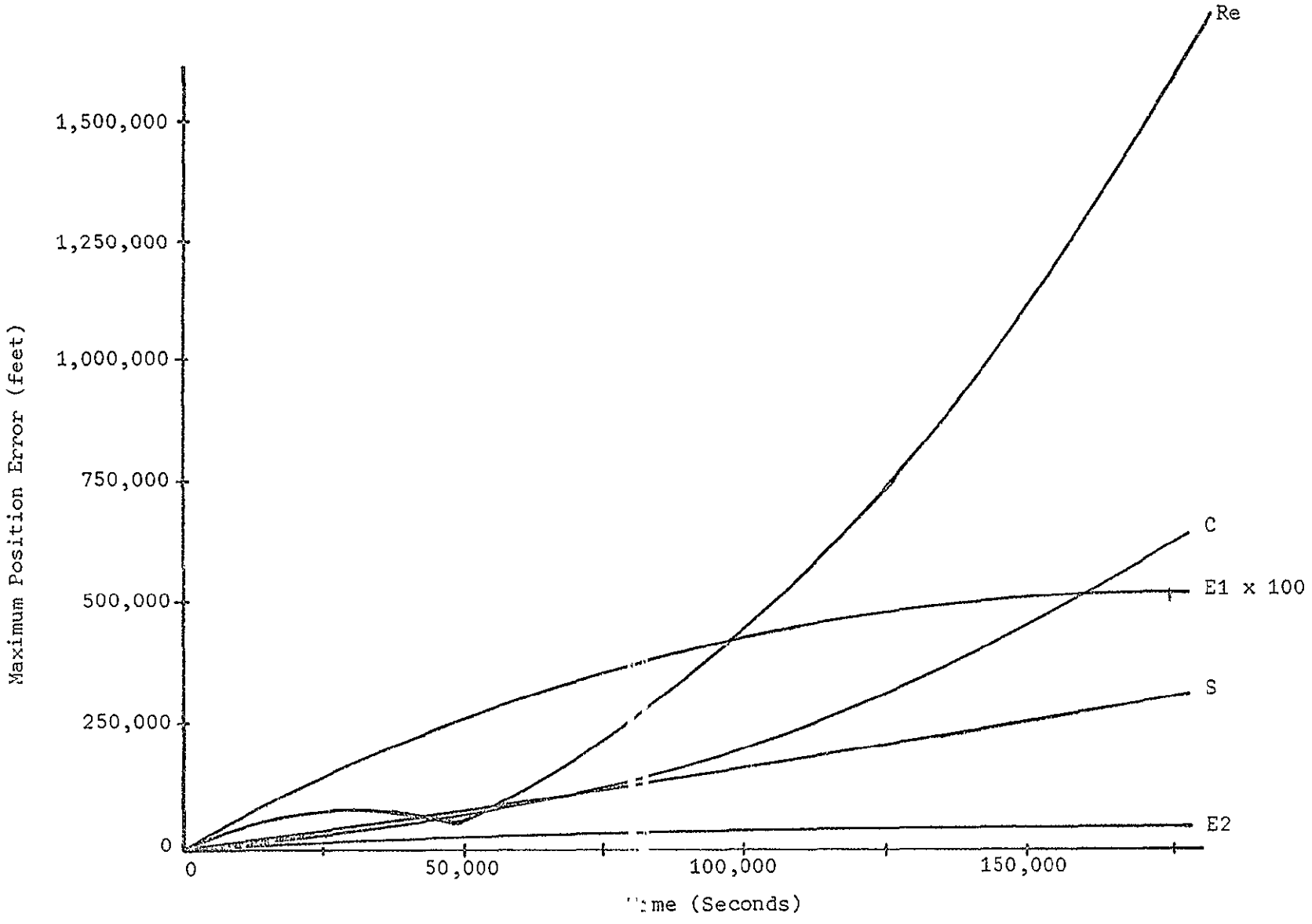

Figure 10. Maximum Position Error, T/P = 10, ISS = 120

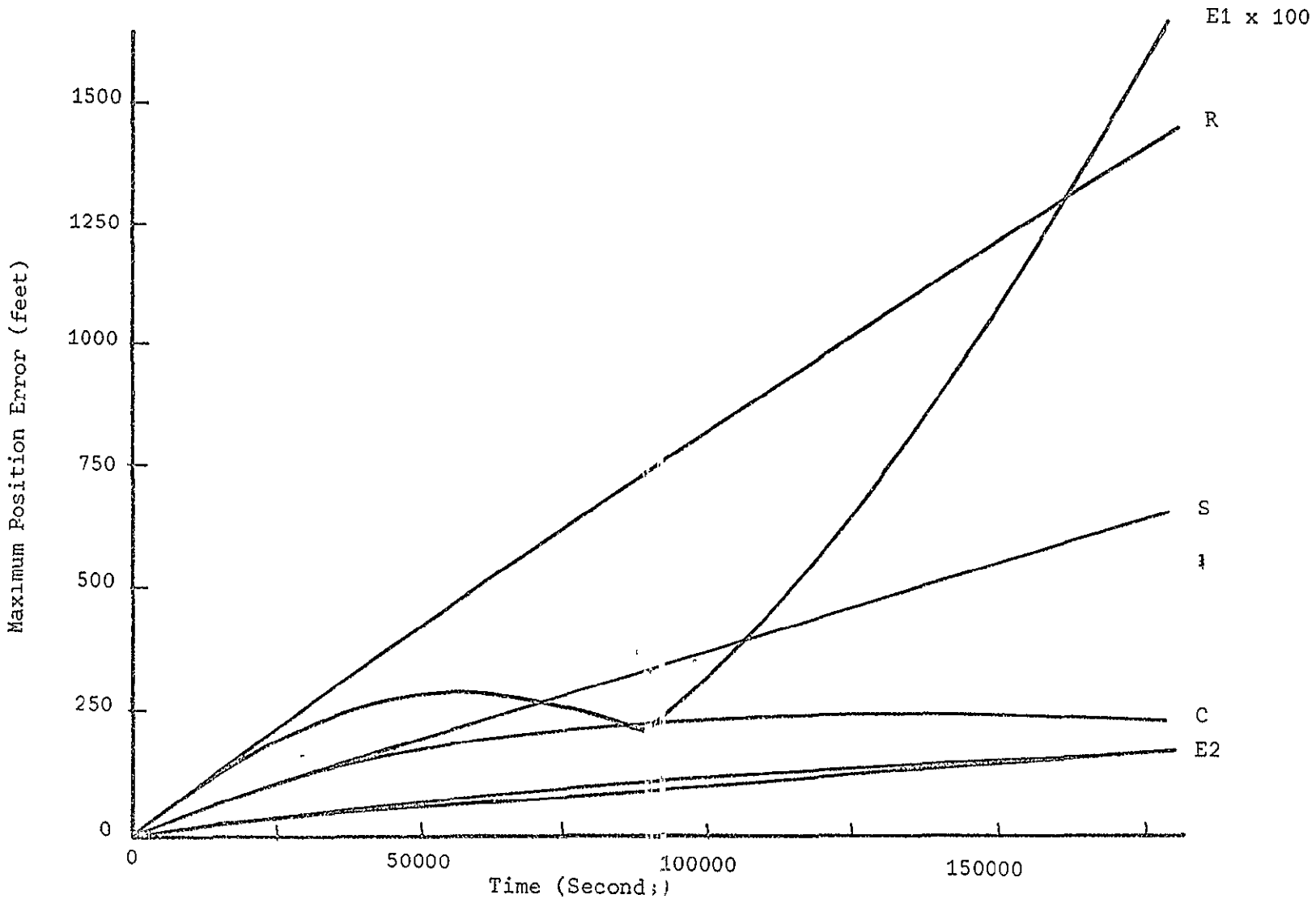

Figure 11. Maximum Position Error, A/P = 5, ISS = 30

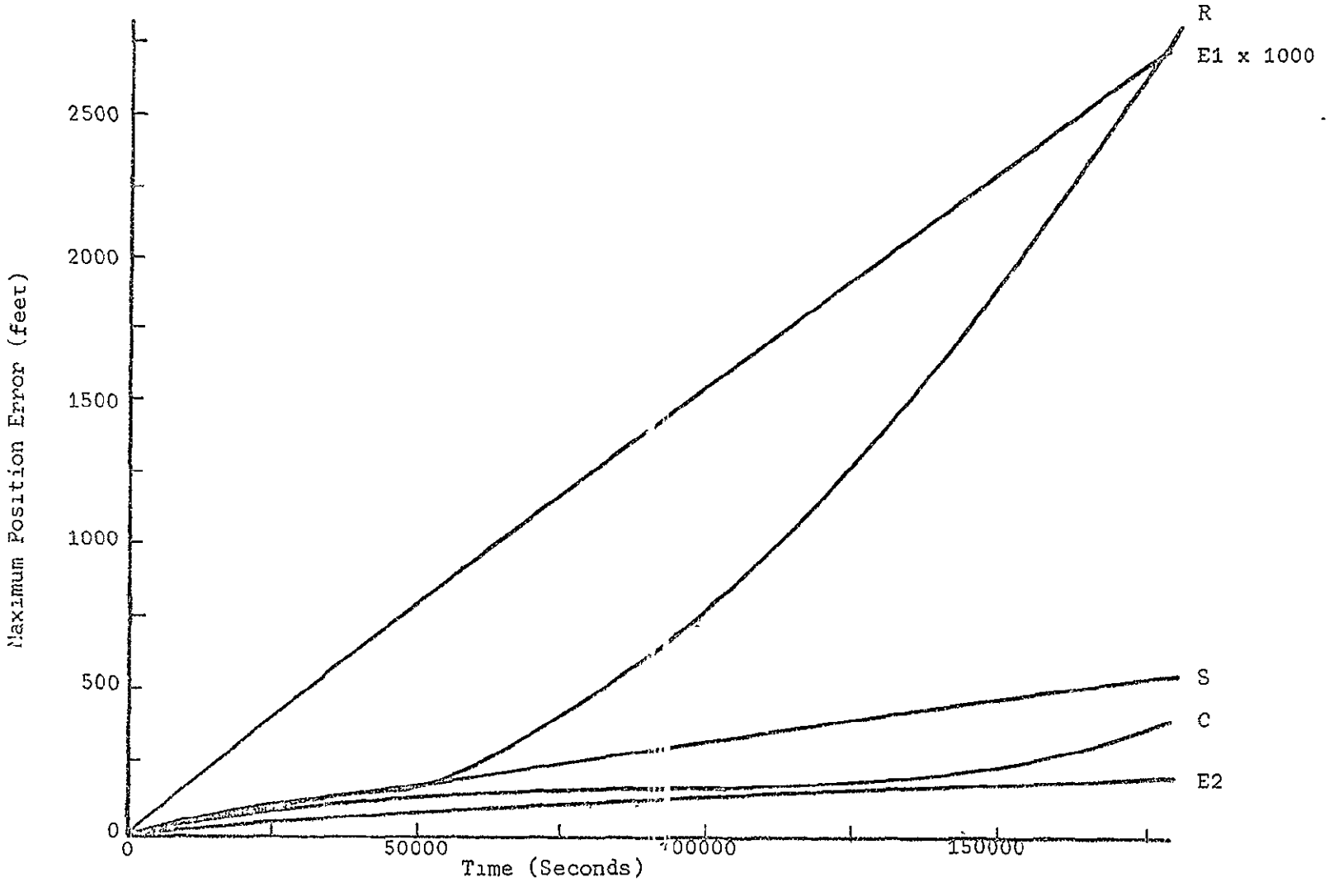

Figure 12. Maximum Position Error, A/P = 2, ISS = 30

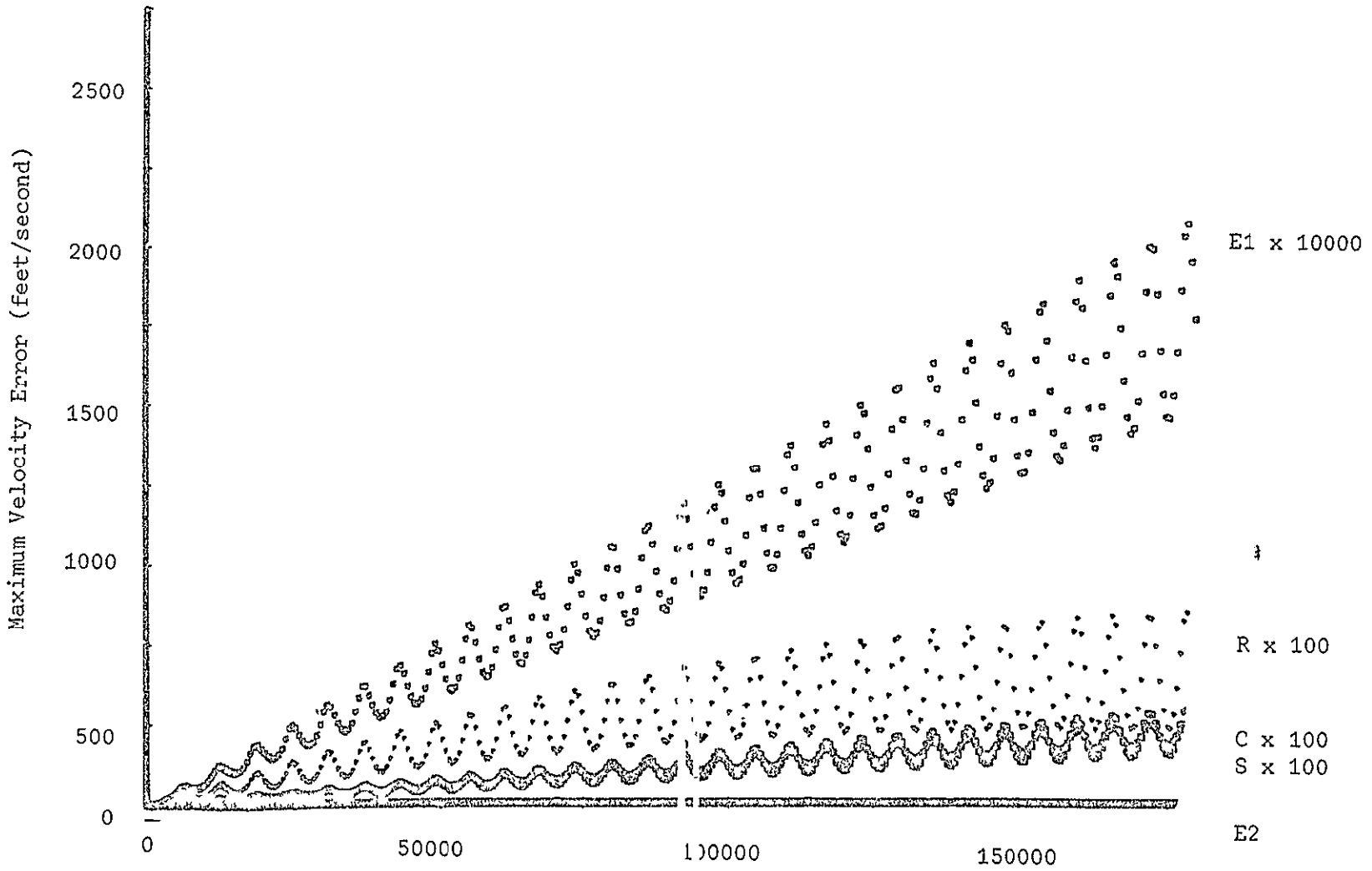

Figure 13 Raw Velocity Error, A/P = 10, ISS = 15

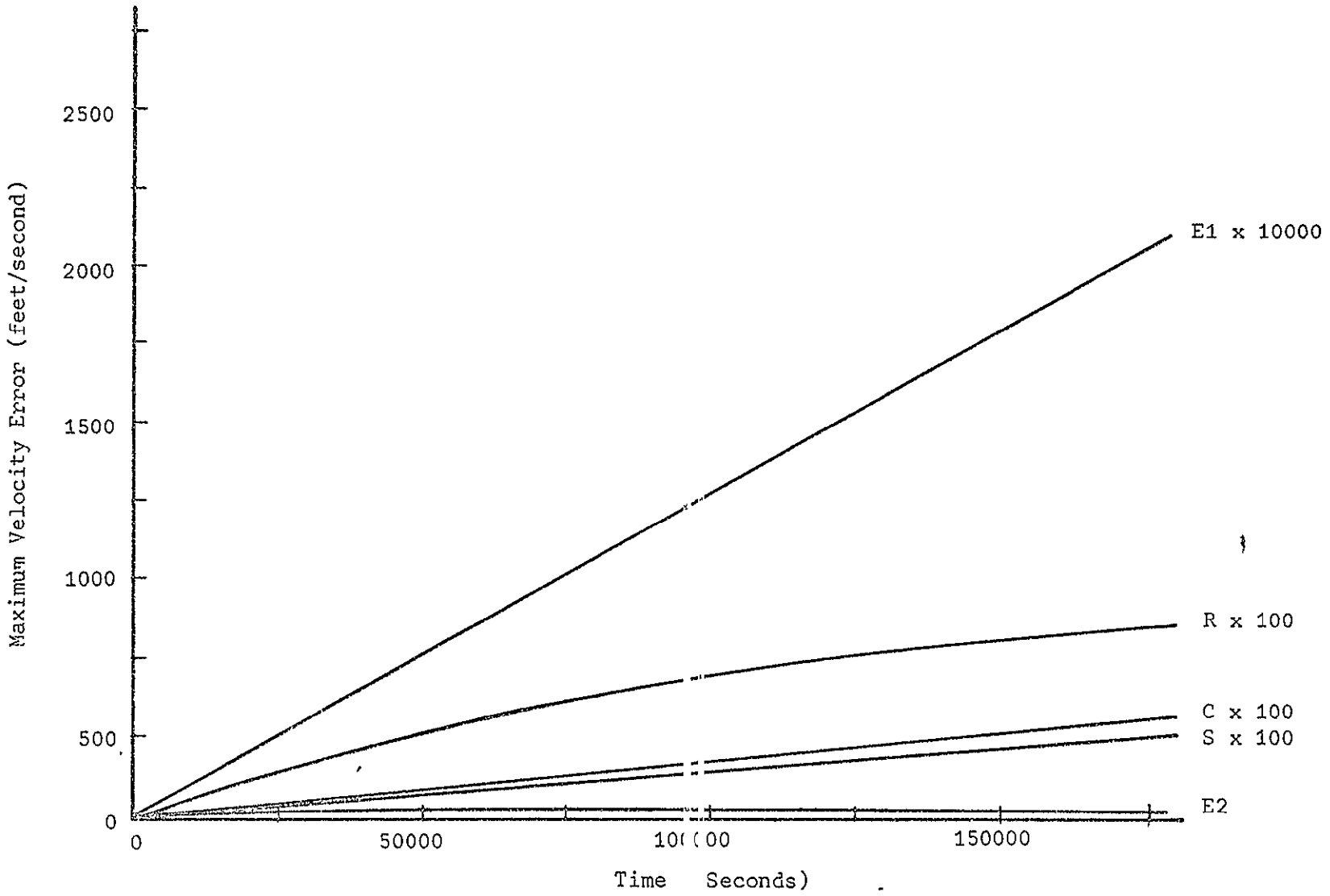

Figure 14. Maximum Velocity Error, ., P = 10, ISS = 15

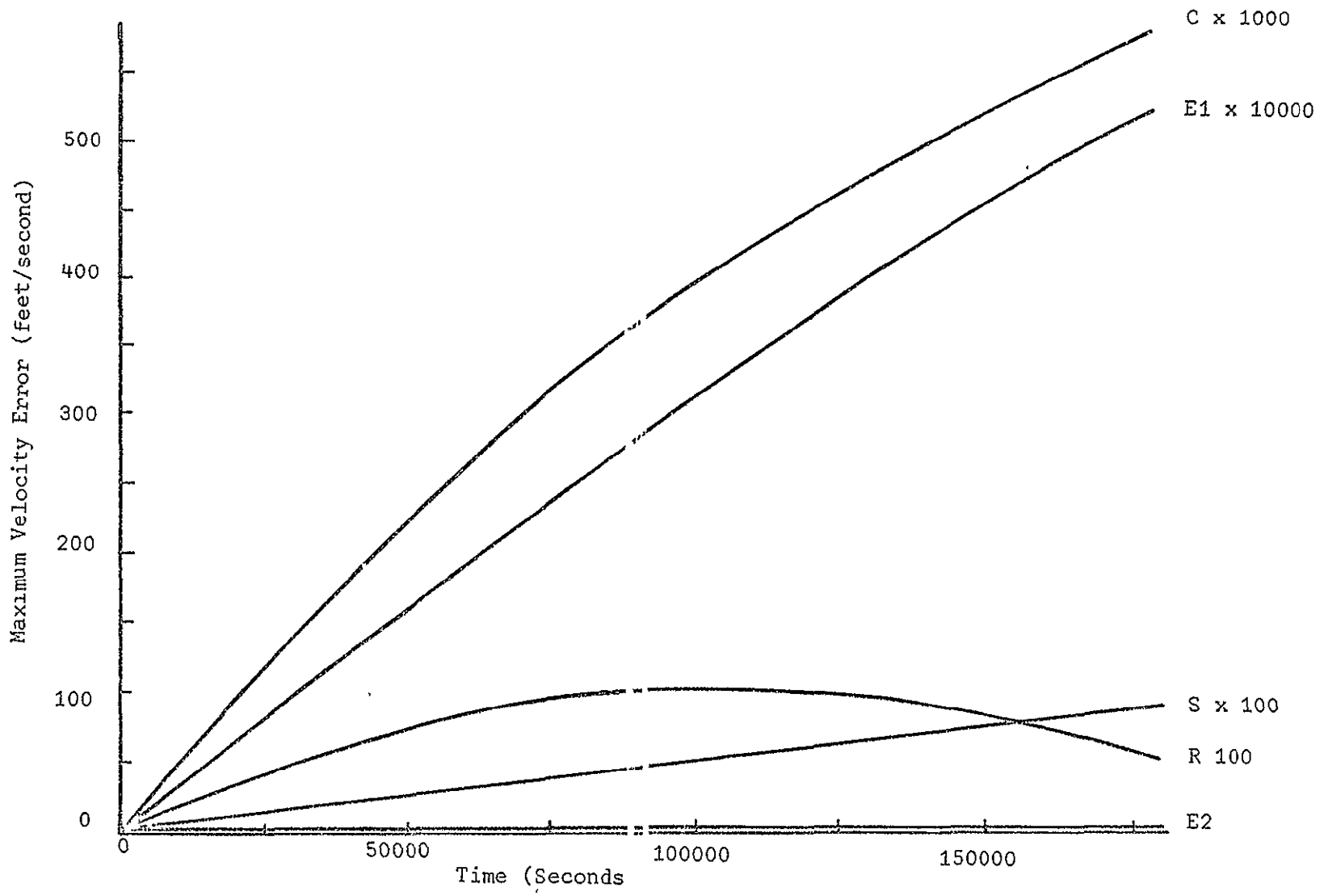

Figure 15. Maximum Velocity Error, A/P = 10, ISS = 30

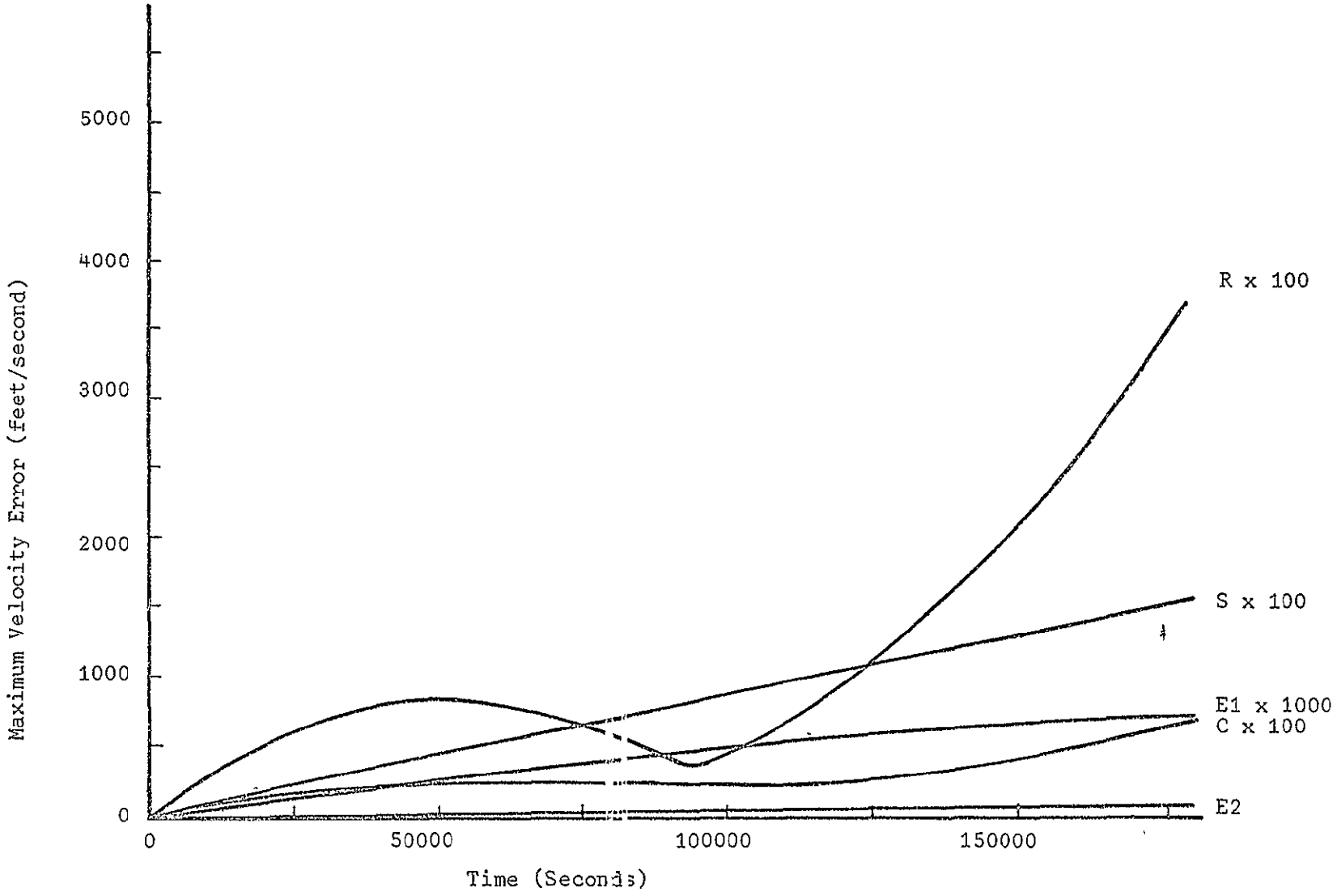

Figure 16. Maximum Velocity Error, A/P = 10, ISS = 60

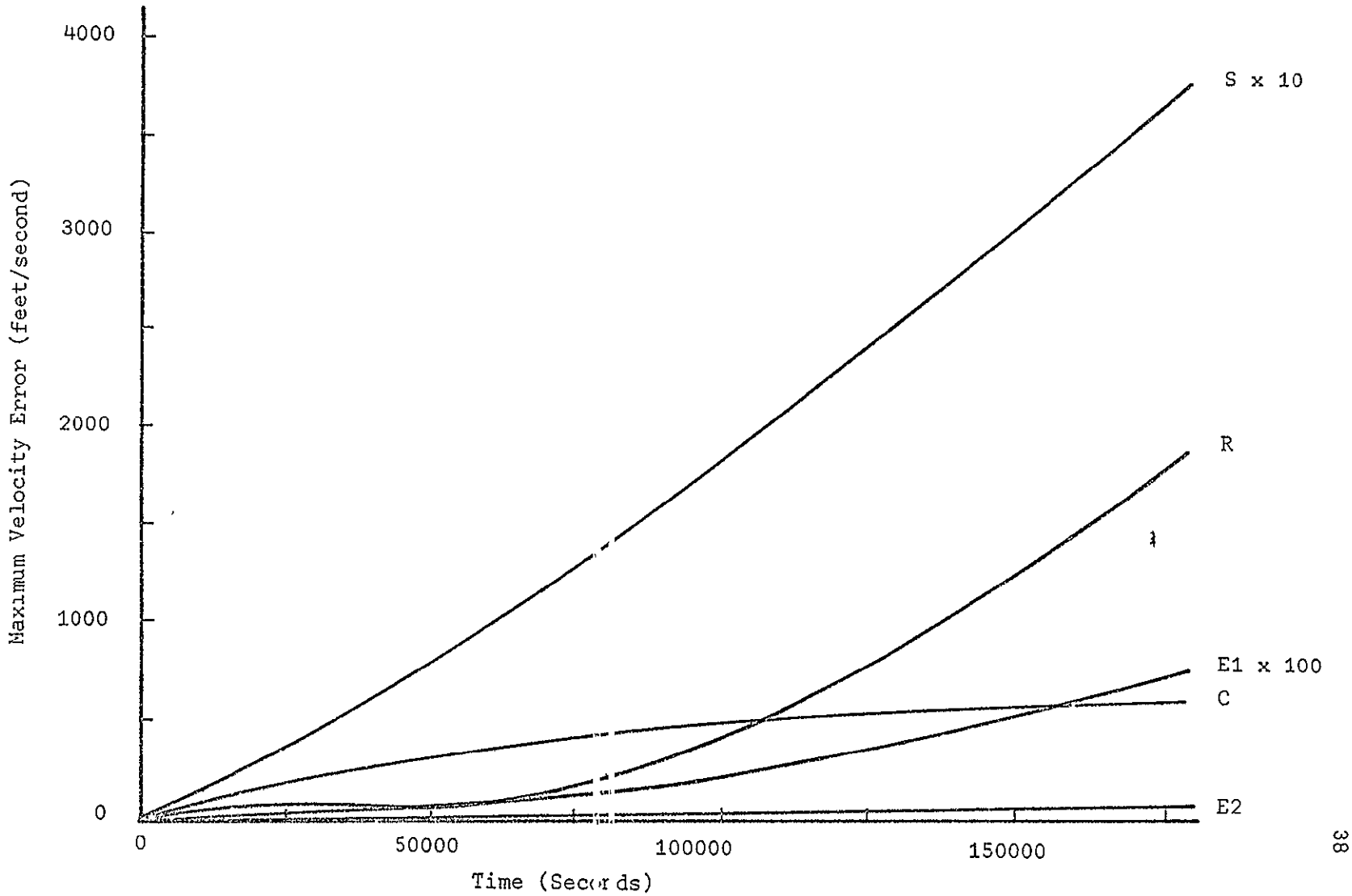

Figure 17. Maximum Velocity Error, A/P = 10, ISS = 60

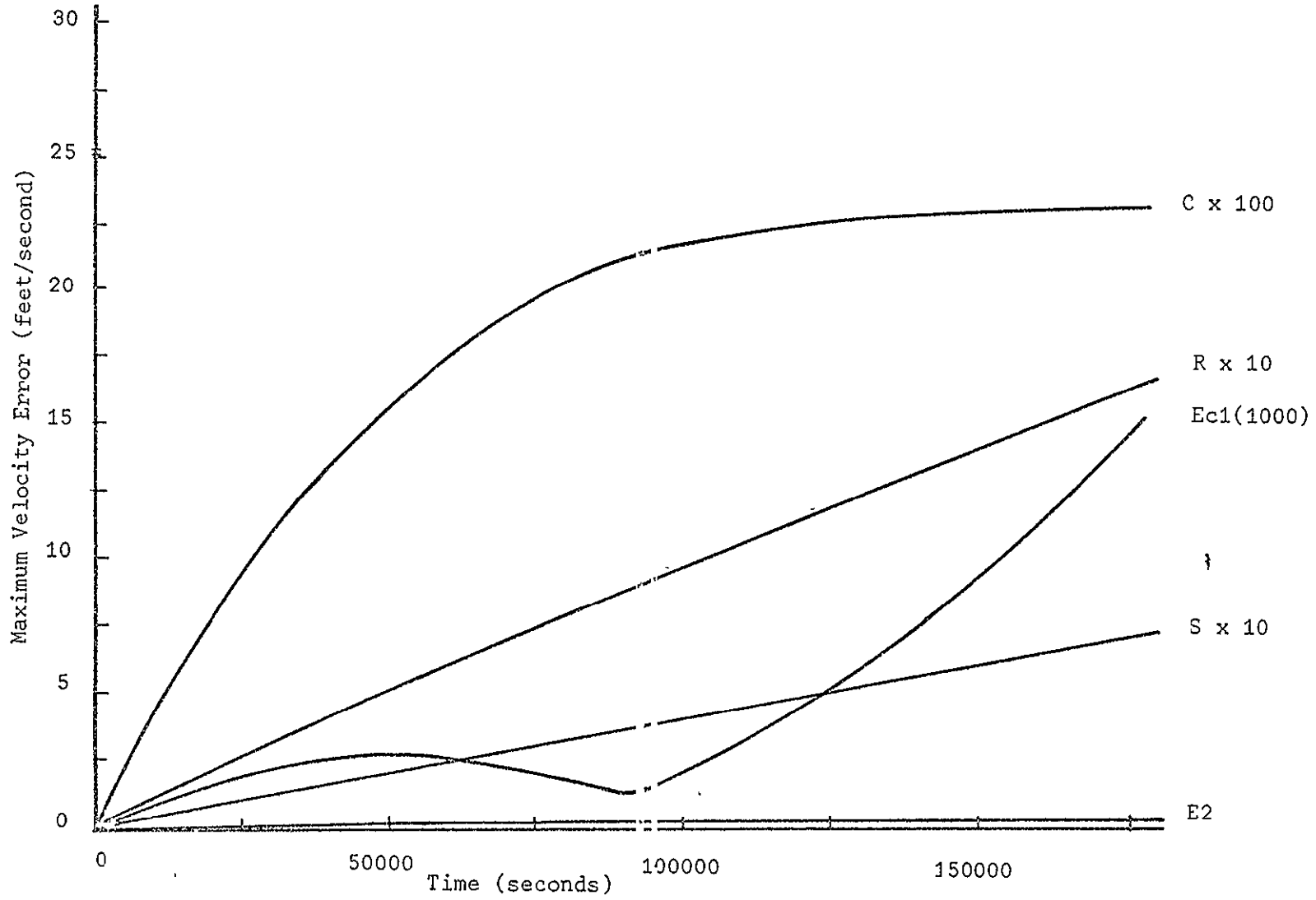

Figure 18. Maximum Velocity Error, A/P = 5, ISS = 30

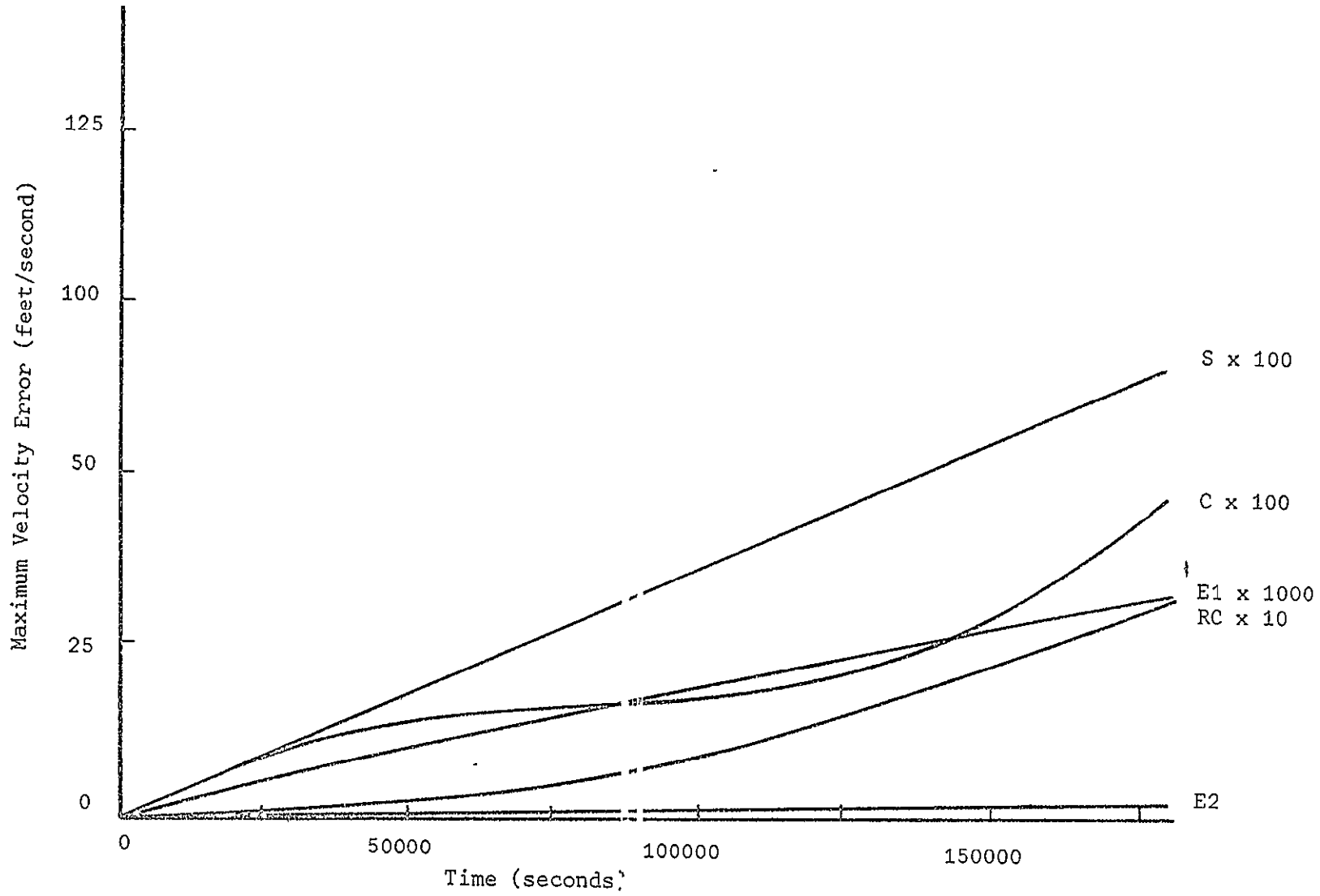

Figure 19. Maximum Velocity Error. A/P = 2, ISS = 30

ELLIPTIC COORDINATES, SET 1, TERMINAL TIME VALUES FOR CIRCULAR ORBITS		
Step Size (seconds).	Position Error (feet)	Velocity Error (feet/second)
15	0.07284	0.00008698
30	0.02406	0.00002873
60	0.02120	0.00002531
120	0.01546	0.00001846
150	0.00309	0.00000369
240	0.00678	0.00000809

TABLE 6

ELLIPTIC COORDINATES TERMINAL TIME COMPARISONS					
Step Size (seconds)	A/P	Position Error (feet)		Velocity Error (feet/second)	
		Set 1	Set 2	Set 1	Set 2
15	2	0.3196	11.2482	0.0004	0.0131
	20	11.3869	12.0965	0.0123	0.0131
30	2	2.7310	175.8160	0.0032	0.2054
	20	167.5230	172.6260	0.1810	0.1920
60	2	40.5700	2691.4200	0.0471	3.2520
	20	2173.8500	1986.0400	0.3484	2.5780
120	2	560.3300	38759.4000	0.6501	55.5405
	20	9792.5600	9142.8400	10.5715	59.9666

TABLE 7

ERROR COMPARISON 15 SEC STEP SIZE					
A/P	R	C	S	E2	E1
	Terminal Time Position Error (feet)				
1	100.910	6.5387	28.3569	12.4850	0.0728
2	77.029	15.6925	33.0283	11.2482	0.3196
5	15.298	28.3731	36.9600	9.9504	1.0695
10	83.986	44.7332	42.9504	8.7478	2.9602
20	271.134	97.8794	52.8845	12.0965	11.3869
Maximum Position Error (feet)					
1	100.910	18.0245	30.8165	17.9850	0.0728
2	77.248	19.7348	33.2170	13.8808	0.3196
5	36.105	33.4939	38.8750	14.6235	1.0695
10	125.670	58.1618	44.1784	90.0689	3.2218
20	271.134	97.8794	52.8845	86.6879	11.3869
Terminal Time Velocity Error (ft/sec)					
1	0.1205	0.0212	0.0367	0.0149	0.00009
2	0.0850	0.0150	0.0367	0.0131	0.00037
5	0.0145	0.0322	0.0431	0.0112	0.00121
10	0.0846	0.0465	0.0455	0.0090	0.00305
20	0.2712	0.1002	0.0591	0.0132	0.01230
Maximum Velocity Error (ft/sec)					
1	0.1205	0.0214	0.0367	1.3083	0.00009
2	0.0850	0.0222	0.0379	2.6678	0.00038
5	0.0331	0.0331	0.0431	2.4131	0.00124
10	0.1218	0.0630	0.0519	51.5267	0.00366
20	0.2712	0.1002	0.0591	14.6945	0.01230

TABLE 8

ERROR COMPARISON FOR 30 SEC STEP SIZE					
A/P	R	C	S	E2	E1
	Terminal Time Position Error (feet)				
1	3415.7800	417.1100	494.0320	172.6260	0.02406
2	2839.1400	385.8500	565.8650	175.8160	2.73115
5	1201.2200	118.0900	626.0040	159.0570	14.06290
10	372.5100	400.5900	709.5340	134.9860	42.59470
20	2920.4300	1203.3400	846.8990	172.6260	167.52200
	Maximum Position Error (feet)				
1	3415.7800	487.1000	529.9230	389.4900	0.02400
2	2839.1400	407.0700	566.7660	326.4700	2.73900
5	1651.3300	246.5800	652.4170	211.4900	14.06300
10	1060.4600	589.0800	733.2990	1039.2900	46.01300
20	2920.4300	1203.3400	846.8990	1373.5400	167.52200
	Terminal Time Velocity Error (ft/sec)				
1	4.0785	0.5864	0.6320	0.2387	0.00003
2	3.2226	0.3842	0.6298	0.2054	0.00317
5	1.4538	0.2175	0.7287	0.1807	0.01595
10	0.3676	0.4303	0.7512	0.1387	0.04382
20	2.8086	1.2096	0.9449	0.1920	0.18098
	Maximum Velocity Error (ft/sec)				
1	4.0785	0.5864	0.6320	42.7050	0.00003
2	3.2226	0.4414	0.6473	119.1500	0.00325
5	1.5252	0.2323	0.7287	30.6480	0.01635
10	0.9935	0.5687	0.8596	581.5750	0.05274
20	2.8170	1.2096	0.9449	230.1740	0.18098

TABLE 9

ERROR COMPARISON FOR 60 SEC STEP SIZE					
A/P	R	C	S	E2	E1
	Terminal Time Position Error (feet)				
1	108908.000	25043.7000	10096.2000	3222.5300	0.02000
2	93982.800	21903.1000	11009.7000	2691.4200	40.57000
5	60304.500	12927.8000	11728.4000	2560.5300	200.91000
10	33929.000	5448.4000	12519.4000	1998.5500	582.38000
20	2060.600	6238.0000	13756.1000	1986.0400	2173.85000
Maximum Position Error (feet)					
1	108908.000	25131.1000	10589.4000	9899.8000	0.02000
2	93982.800	21903.1000	11009.7000	13213.5000	40.57000
5	64143.200	14619.0000	12014.7000	54164.9000	200.91000
10	40482.500	8070.5000	13095.0000	20967.4000	635.33000
20	22929.800	6493.0000	13756.1000	20334.2000	2173.85000
Terminal Time Velocity Error (ft/sec)					
1	130.034	30.2844	12.5889	3.8593	0.00003
2	107.814	24.7957	12.3223	3.2326	0.04707
5	69.674	15.4015	13.5759	2.9181	0.22788
10	35.999	6.4585	13.2545	2.0487	0.59914
20	5.972	5.1896	15.3152	2.5780	2.34835
Maximum Velocity Error (ft/sec)					
1	130.034	30.28440	12.5889	1590.2700	0.00003
2	107.814	24.79570	12.5631	7419.3900	0.04827
5	69.674	15.40150	13.5759	216.8600	0.23411
10	36.344	6.45846	15.2794	5793.7300	0.72210
20	22.150	5.79800	15.2794	2920.7800	2.34835

TABLE 10

ERROR COMPARISON FOR 120 SEC STEP SIZE					
A/P	R	C	S	E2	E1
	Terminal Time Position Error (feet)				
1	3064172.00	1278348.000	379119.000	53863.1000	0.02000
2	2708974.00	1127995.000	364646.000	38759.4000	560.32600
5	2059712.00	856197.000	339097.000	42396.6000	2205.58000
10	1586616.00	628725.000	301231.000	24741.3000	4765.60000
20	1592896.00	547540.000	231853.000	9142.8400	9792.56000
	Maximum Position Error (feet)				
1	3064172.00	1278348.000	380589.000	594284.0000	0.02000
2	2708974.00	1127995.000	364646.000	243501.0000	564.63000
5	2059712.00	856197.000	339097.000	197259.0000	2205.58000
10	1619416.00	649060.000	322389.000	175354.0000	5268.40000
20	1592896.00	547540.000	231853.000	195278.3000	12389.52000
	Terminal Time Velocity Error (ft/sec)				
1	3656.20	1527.040	456.104	85.0721	0.00002
2	3116.62	1298.000	416.088	55.5405	0.65011
5	2344.99	975.208	386.801	49.0478	2.50149
10	1670.24	661.111	317.481	25.5778	4.90396
20	1809.25	616.306	256.427	59.9667	10.57150
	Maximum Velocity Error (ft/sec)				
1	3656.20	1527.040	456.104	12324.3000	0.00002
2	3116.62	1298.670	418.667	9012.9000	0.66885
5	2344.99	975.210	386.801	15553.2000	2.59316
10	1896.08	761.480	372.830	41486.6000	5.98710
20	1809.25	616.310	256.427	12112.5000	10.57150

TABLE 11

data, only the plots showing the maximum error envelopes will be shown for the remaining data. However in discussing the results, reference will still be made to the oscillation in the error curves. The amplitudes of these periodic deviations increase for both step size increases (constant eccentricity) and eccentricity increases (constant step size).

III.1 Effect of Step Size on Error Propagation

In analyzing the data generated in this investigation for step size effects (Figures 7, 8, and 9), one characteristic immediately noticeable is that the error plots for each coordinate system are oscillatory in nature with a period corresponding to that of the orbit as is shown in Figure 6. Closer examination reveals that the amplitudes of oscillation are dependent on the integration step size for constant orbit shape. This dependence is such that as the step size increases, the oscillation amplitude also increases. With but one exception, all of the coordinate error curves exhibit this type of periodic deviations superimposed upon nearly linear increasing functions of orbit time. The rectangular coordinate errors increase in a nonlinear fashion with large periodic deviations. In the following paragraphs the relative influence of step size on each coordinate system is discussed.

The nonlinear characteristic of the average rectangular coordinate error curves indicate that this system is indeed sensitive to integration step size. The rectangular coordinate error

usually increases slowly with orbit time for the smaller step sizes (constant eccentricity) as shown in Figure 6 or 7. As the integration interval increases, the rectangular coordinate error reaches a local maximum (Figure 8) and then declines to a local minimum. Upon passing through this local minimum, the state deviations increase almost exponentially (Figure 9). Increasing the step size further causes the local maximum and minimum to be reached much earlier in time (Figure 10) thus allowing more time for terminal error buildup. This trend is not as apparent in the other integration error curves, although the errors in the circular coordinate system exhibit a greater step size dependence than do the spherical coordinate errors.

In comparing the circular coordinate errors to the spherical coordinate errors, it is apparent that the errors which occur in the spherical system are generally larger than those which occur in the circular system for the 15 and 30 second step sizes and small eccentricities as shown in Figures 8, 11, and 12. However, for the larger eccentricities the spherical error curve approximates the average circular error curve (Figure 6). For these cases, the circular error curve exhibits large deviations about the average curve. For the larger step sizes, 60 and 120 seconds, the spherical deviations are larger than the circular errors early in the accumulated integration time. This occurs prior to the buildup of truncation error resulting from too large a step size (Figure 10). As the effects of truncation error increase, the circular errors become larger than the

spherical coordinate errors as is expected. This effect leads to the conclusion that circular coordinate errors are more sensitive to step size than either the spherical or elliptic coordinate errors.

The coordinate errors in the elliptic coordinates, sets 1 and 2 (as defined in Equations 5 and 6, respectively), generally increase only slightly as the step size increases are made. Coordinate set 2 exhibits a greater error sensitivity (error increase) to step size for all orbit shapes than does coordinate set 1. In addition, the scattering of a few data points (the few extremely large deviations from the average error curve - see Figures 6 and 13) in set 2 increases in magnitude as the step size increases. The few scattered points were not considered in the determination of the maximum error envelopes for set 2. Coordinate set 1 appears to be only slightly sensitive to step size with the errors increasing more for the larger eccentricities. Furthermore, coordinate set 1 does not exhibit any data scatter. An exception to the error increase with step size increase is noted for circular orbits. As the step size increases, the state deviations decrease. Further investigation shows that the errors in the state decrease to a minimum between the step size of 120 seconds and 240 seconds. Note that the terminal time comparisons given in Table 6 are valid, since for circular orbits, the errors of the elliptic cylinder coordinates, set 1, increase without oscillation. This indicates that the "best" (most accurate) step size for circular orbits exists in the step size range

of 120 to 240 seconds for the CDC 6600 Computer. The decrease in state errors for step size increases is evidently due to a reduction in round-off error resulting from fewer integrations. The state error increases for the larger step sizes must be due then to truncation error. Note that none of the other coordinate systems investigated indicates the existence of a "best" step size in the range considered (15 seconds to 120 seconds) regardless of orbit shape. It follows then that the "best" step size for any of the other coordinate systems considered (if it exists) must be less than 15 seconds. This indicates that the "best" step size (maximum accuracy) depends upon the word length of the computer involved with the larger word lengths allowing the most accuracy in the integrated states. This hypothesis is further supported by that fact that Gerber and Lewallen[1] found that for circular orbits a best step size of 30 seconds existed for the spherical coordinate system for the Univac 1108.

In general then, as the integration step size increases, both the position and velocity errors increase for all combinations of coordinate system, orbit shape and step size. The lone exception is for circular orbits using set 1 of the elliptic coordinates as previously mentioned.

III.2 Effect of Orbit Shape on Error Propogation

In examining the plotted data for eccentricity effects, it is observed that the error curves, in addition to being step size dependent, are also eccentricity dependent. The state deviations

display small amplitudes for small eccentricities (constant step size) and approximate a smooth curve for circular orbits. As the eccentricity increases, the amplitudes also increase with the rectangular coordinate system exhibiting the largest increase.

The amplitudes of the oscillating rectangular coordinate errors are highly eccentricity dependent increasing significantly as the eccentricity increases. In addition to influencing the error curve amplitudes, the eccentricity increases affect the average error curve in a reverse manner to that of the step size variations. In this case, as the eccentricity increases (constant step size), the local maximum and minimum begin to appear later in orbit time (Figures 8, 11, and 12). However, an increase in the amplitude of the periodic deviations keeps the state errors large. This trend probably results from the fact that the coordinates vary more slowly for the larger orbits than for the smaller orbits.

A close examination of the effect of orbit shape upon the spherical and circular coordinate error curves indicates that both of these systems are affected in a similar manner. This conclusion is based on the fact that early in the orbit time, when step size influence is minimal, the spherical coordinate errors are usually larger than the circular coordinate errors. As truncation error influence (due to large step size) increases, the circular errors become larger than the corresponding spherical errors (Figure 10). This trend continues for nearly all eccentricities. Thus, it is concluded that eccentricity does not appear to influence the state

deviations in the spherical and circular coordinate systems to a high degree. This same conclusion can be extended to the elliptic coordinates.

The elliptic coordinates, sets 1 and 2, both appear to be the coordinate systems the least influenced by eccentricity changes. Set 2 continues to exhibit scattered data points in the vicinity of apogee. Coordinate set 1 appears to be slightly more sensitive to eccentricity due to the fact that the magnitude of the terminal position errors increases significantly as eccentricity increases. Table 7 compares state errors at the terminal time for both systems indicating to a degree the sensitivity of each to eccentricity. However, note that the terminal time comparisons are not completely valid due to the oscillating nature of the error curves. Note also that although both coordinate sets have approximately the same error, set 1 would still be more desirable computationally because its error envelope is much smaller than that for set 2.

It may thus be concluded that all the coordinate error curves are influenced by eccentricity. This influence though, is not as strong as that due to step size.

III.3 Effect of Coordinate System on Error Propagation

The effect of coordinate system alone upon the errors in state is indeed difficult to isolate due to the interaction of the orbit shape and the integration step size. In the paragraphs to follow, each coordinate system will be separately discussed, and the

respective advantages or disadvantages given.

The rectangular coordinate system is highly sensitive to step size and eccentricity. Generally speaking the error magnitudes become quite large and dominate the error magnitudes in all the other coordinate systems considered. This is evident in Tables 8, 9, 10, and 11 which compare terminal time error with the largest error occuring during the integration interval. Due to the large errors the rectangular coordinate system is not recommended for numerical studies.

The circular coordinate system is also sensitive to increases in step size and orbit shape as indicated in Tables 8, 9, 10, and 11. Although the circular coordinate errors are small in some instances, the large periodic oscillating error curves generally mean large state errors. A comparison of the circular coordinate errors with those obtained using spherical coordinates indicates that both systems have potential uses depending upon the type of orbit to be investigated and the step size to be taken.

The spherical coordinate state deviations are quite stable and do not vary drastically for step size changes (see Tables 8, 9, 10, and 11). Orbit shape appears to have little effect on coordinate errors in this system. The stability of this system indicates that it may be very useful for investigating perturbed orbits.

The elliptic coordinate systems produce the most accurate states (Tables 8, 9, 10, and 11). The scattering of isolated data points in coordinate set 2 is highly undesirable. Coordinate set 1,

however, is generally quite accurate. In addition this system also appears to be a desirable one in which to investigate perturbed motion. One possible objection to this system as used here, is that the system is rectified to the orbit plane. This requires a coordinate transformation to obtain the inertial states. However, the accuracy gained more than outweighs this disadvantage. It thus appears that the elliptic cylinder coordinates, set 1, offer superior computational accuracy and exhibit computational stability over long time intervals even for large step sizes.

CHAPTER IV

CONCLUSIONS AND RECOMMENDATIONS

IV.1 Summary

The sensitivity of two body states obtained through numerical integration to coordinate system and integration step size is investigated for various orbit types. This is accomplished by numerically integrating the equations of two-body motion for the various coordinate systems and then comparing resulting states to the states generated through the two-body solution. By holding one parameter constant and varying the other two, the effect of each on the integrated states can be determined. It is observed that for all coordinate systems considered in this investigation, step size has a greater influence on the error than the orbit shape. This may be seen by comparing Figures 7, 8, and 9 to Figures 8, 11, and 12. Also, it can be observed that the position and velocity error curves behave in a similar manner. This is best seen by comparing Figure to Figure . Finally, any operation designed to reduce the errors in position also reduces the errors in velocity as is evidenced by the corresponding decreases in position and velocity errors of the elliptic cylinder coordinates (Tables 8, 9, 10, and 11).

IV.2 Conclusions

Based on the data generated in this investigation the following conclusions have been reached. Some of these conclusions are made with reservations since additional investigation is necessary before final conclusions are possible.

1. Elliptic coordinates, set 1, exhibit superior computational accuracy when compared to the other coordinate systems. This system remains relatively insensitive to orbit shape and integration step size as far as error increases are concerned. The error curve increases in a linear manner, and the periodic variations superimposed on the average error curve are generally quite small. The amplitude of the periodic deviations increases only slightly, thereby providing a small error envelope.

2. Elliptic coordinates, set 1, allow much larger step sizes to be taken before similar error magnitudes occur. These large step sizes represent a cost decrease by reducing the running time.

3. Elliptic coordinates, set 2, also produce error curves whose magnitudes are quite small. However, the isolated scatterer error points cause the error envelope to become quite large. This is the only unattractive feature of this system. Note, however, that even without the isolated scatter of error points, set 1 is still more accurate than set 2.

4. Given the option of choosing from a set of coordinate systems, one containing the angle itself and the other containing the cosine of the angle as one of the coordinates, the set containing the angle should be chosen. Integration of the angle is inherently more accurate than integration of the cosine since the angle increases monotonically while the cosine is oscillatory. This is verified by comparing the results of elliptic coordinates, set 1, to elliptic coordinates, set 2. Both sets are identical in all respects except

that in set 1 the angle is integrated while in set 2 the cosine of the angle is integrated. Thus, any difference in error magnitudes between the two systems must result from the integration of the cosine.

5. The spherical coordinate error curves are well behaved and increase linearly with time. Periodic deviations of almost constant amplitude are superimposed on the average error curve for all combinations of orbit shape and step size. The small periodic deviations about the linear average error curve is a desirable feature of this system because the small deviations keep the error envelope small thereby allowing the actual error curve to be approximated by the average error curve.

6. The circular coordinate errors vary in magnitude according to step size and orbit shape. Depending upon the step size and orbit shape, the coordinate errors either remain small or increase rapidly with large periodic deviations which cause the error envelope to become quite large. This type of error propagation is the undesirable feature associated with using this coordinate system.

7. For small step sizes (15 and 30 seconds) and small orbits (A/P = 1, 2, 5), the circular coordinate errors are usually smaller than the spherical state deviations. For large orbits (A/P = 5, 10, 20) and both large and small step sizes, the spherical coordinate coordinate errors are generally smaller than the circular state errors.

8. Rectangular coordinate error curves are greatly influenced by step size and orbit shape and usually produce extremely large errors.

These large errors are the results of either the large periodic variations (large error envelope) superimposed on the average error curve or the nonlinear (exponential type) increase of the average error curve.

9. The "best" step sizes (those step sizes for which the integrated states are the most accurate) appear to be dependent upon coordinate system and computer word length.

IV.3 Recommendations

The following recommendations for further study are made:

1. Similar data should be generated on other computers in order to determine how step size as a function of word length effects the accuracy of the integrated states.

2. A thorough study in which other coordinate systems than those considered in this study are included should be made for a wider range of integration step sizes and orbit shapes. The computation involved should be done on several different computers using both single and double-precision arithmetic in order to determine the effect machine and arithmetic type on the accuracy of the integrated states.

APPENDICES

APPENDIX A

The transformations between coordinate systems as used in this study are presented in the following sections.

A.1 Transformations Between Spherical and Rectangular Coordinates

Spherical to Rectangular

$$X = \rho \cos\sigma \cos\tau \qquad Y = \rho \cos\sigma \sin\tau \qquad Z = \rho \sin\sigma \tag{1}$$

and by differentiation

$$\begin{aligned} \dot{X} &= \dot{\rho}\cos\sigma\cos\tau - \rho\,\dot{\sigma}\sin\sigma\cos\tau - \rho\,\dot{\tau}\cos\sigma\sin\tau \\ \dot{Y} &= \dot{\rho}\cos\sigma\sin\tau - \rho\,\dot{\sigma}\sin\sigma\sin\tau + \rho\,\dot{\tau}\cos\sigma\cos\tau \\ \dot{Z} &= \dot{\rho}\sin\sigma + \rho\,\dot{\sigma}\cos\sigma \end{aligned} \tag{2}$$

Rectangular to Spherical

Again, from geometry

$$\begin{aligned} \rho &= (X^2 + Y^2 + Z^2)^{\frac{1}{2}} \\ \tau &= \tan^{-1}(Y/X) \\ \sigma &= \tan^{-1}(Z/(X^2 + Y^2)^{\frac{1}{2}}) \end{aligned} \tag{3}$$

and by differentiation

$$\dot{\rho} + \frac{X\dot{X} + Y\dot{Y} + Z\dot{Z}}{(X^2 + Y^2 + Z^2)^{\frac{1}{2}}}$$

$$\dot{\tau} = \frac{X\dot{Y} - Y\dot{X}}{(X^2 + Y^2)} \tag{4}$$

$$\dot{\sigma} = \frac{(X^2 + Y^2)\dot{Z} - Z(X\dot{X} + Y\dot{Y})}{(X^2 + Y^2)^{\frac{1}{2}}\,(X^2 + Y^2 + Z^2)}$$

A.2 Transformations Between Circular and Rectangular Coordinates

Circular to Rectangular

From Figure 4,,

$$X = r \cos \theta \qquad Y = r \sin \theta \qquad Z = z \tag{5}$$

and by differentiation, the velocity transformations become

$$\begin{aligned} \dot{X} &= \dot{r} \cos \theta - r \dot{\theta} \sin \theta \qquad \dot{Y} = \dot{r} \sin \theta + r \dot{\theta} \cos \theta \\ \dot{Z} &= \dot{z} \end{aligned} \tag{6}$$

Rectangular to Circular

Again, from geometry,

$$r = (X^2 + Y^2)^{\frac{1}{2}} \qquad \theta = \tan^{-1} (Y/X) \qquad z = Z \tag{7}$$

and by differentiation the velocity transformations become

$$\dot{r} = \frac{X\dot{X} + Y\dot{Y}}{(X^2 + Y^2)^{\frac{1}{2}}} \qquad \dot{\theta} = \frac{X\dot{Y} - Y\dot{X}}{X^2 + Y^2} \qquad \dot{z} = \dot{Z} \tag{8}$$

A.3 Transformations Between Elliptic Coordinates, Set 1, and Rectangular Coordinates

Elliptic Coordinates, Set 1, To Rectangular

$$\begin{aligned} X &= \alpha_1 \cos \alpha_2 - ae \qquad Y = \alpha_1 (1 - e^2)^{\frac{1}{2}} \cos \alpha_2 \\ Z &= \alpha_3 \end{aligned} \tag{9}$$

and by differentiation

$$\dot{X} = \dot{\alpha}_1 \cos \alpha_2 - \alpha_1 \dot{\alpha}_2 \sin \alpha_2$$

$$\dot{Y} = \dot{\alpha}(1 - e^2)^{\frac{1}{2}} \sin \alpha_2 + \alpha_1 \dot{\alpha}_2 (1 - e^2)^{\frac{1}{2}} \cos \alpha_2 \qquad (10)$$

$$\dot{Z} = \dot{\alpha}_3$$

Rectangular to Elliptic Coordinates, Set 1

$$\alpha_1 = a \qquad \alpha_2 = E \qquad \alpha_3 = 0 \qquad (11)$$

and by differentiation

$$\dot{\alpha}_1 = 0 \qquad \dot{\alpha}_2 = \dot{E} \qquad \dot{\alpha}_3 = 0 \qquad (12)$$

A.4 Transformations Between Elliptic Coordinates, Set 2, and Rectangular Coordinates

Elliptic Coordinates, Set 2, to Rectangular

$$X = \beta_1 \beta_2 - a\, e \qquad Y = \beta_1 (1 - e^2)^{\frac{1}{2}} (1 - \beta_2^2)^{\frac{1}{2}} \qquad Z = \beta_3 \qquad (13)$$

and by differentiation

$$\dot{X} = \dot{\beta}_1 \beta_2 + \beta_1 \dot{\beta}_2 \qquad \dot{Y} = \frac{\dot{\beta}_1 [(1 - e^2)(1 - \beta_2^2)]^{\frac{1}{2}} Y - \beta_1^2 \beta_2 \dot{\beta}_2 (1 - e^2)}{Y} \qquad (14)$$

$$\dot{Z} = \dot{\beta}_3$$

Note that $\dot{Y}$ does not exist for Y equal zero and must be determined by another method ($\overline{h} = \overline{r} \times \overline{v}$). Note also that the proper sign for Y is ambiguous and must be determined from considerations of X and $\dot{X}$.

Rectangular to Elliptic Coordinates, Set 2

$$\beta_1 = z \qquad \beta_2 = \cos E \qquad \beta_3 = 0 \tag{15}$$

and by differentiation

$$\dot{\beta}_1 = 0 \qquad \dot{\beta}_2 = -\dot{E} \sin E \qquad \dot{\beta}_3 = 0 \tag{16}$$

A.5 Transformation From the Orbital Plane to the Reference Coordinate System

The transformation from orbital elements to the inertial rectangular coordinate system is well known and is derived by various authors. The transformation will not be derived here but is given as obtained from Reference 1

$$\begin{bmatrix} X \\ Y \\ Z \end{bmatrix}_{\text{Inertial}} = \begin{bmatrix} a_{11} & a_{12} & a_{13} \\ a_{21} & a_{22} & a_{23} \\ a_{31} & a_{32} & a_{33} \end{bmatrix} \begin{bmatrix} x \\ y \\ z \end{bmatrix}_{\substack{\text{Orbital} \\ \text{Plane}}} \tag{17}$$

where

$$a_{11} = \cos \omega \cos \Omega - \cos i \sin \Omega \sin \omega$$

$$a_{12} = - \sin \omega \cos \Omega - \cos i \sin \Omega \cos \omega$$

$$a_{13} = \sin i \sin \Omega$$

$$a_{21} = \cos \omega \sin \Omega + \cos i \cos \Omega \sin \omega$$

$$a_{22} = - \sin \omega \sin \Omega + \cos i \cos \Omega \cos \omega$$

$$a_{23} = - \sin i \cos \Omega$$

$$a_{31} = \sin \omega \sin i$$

$$a_{32} = \cos \omega \sin i$$

$$a_{33} = \cos i$$

the angles i, Ω and ω are the orbit inclination, the longitude of the ascending note and the argument of perigee respectively. The coordinates x, y and z are given by

$$x = a \cos E - a e \qquad y = b \sin E \qquad z = 0 \tag{18}$$

APPENDIX B

EQUATIONS OF MOTION

The equations of motion as used in this study are presented in the following sections.

B.1 Rectangular Coordinates

$$\ddot{X} = \frac{-\mu X}{r^3} \qquad \ddot{Y} = \frac{-\mu Y}{r^3} \qquad \ddot{Z} = \frac{-\mu Z}{r^3} \tag{1}$$

where $r = (X^2 + Y^2 + Z^2)^{\frac{1}{2}}$

B.2 Spherical Coordinates

$$\ddot{\rho} = \frac{-\mu}{\rho^2} + \rho\dot{\tau}^2 \cos^2\sigma + \rho\dot{\sigma}^2$$

$$\ddot{\tau} = 2\dot{\tau}\dot{\sigma} \tan\sigma - 2\dot{\rho}\dot{\tau}/\rho \tag{2}$$

$$\ddot{\sigma} = -\dot{\tau}^2 \cos\sigma \sin\sigma - 2\dot{\rho}\dot{\sigma}/\rho$$

B.3 Circular Coordinates

$$\ddot{\rho} = -\frac{\rho\mu}{(\rho^2 + z^2)^{3/2}} + \rho\dot{\theta}^2 \qquad \ddot{\theta} = -\frac{2\dot{\rho}\dot{\theta}}{\rho} \qquad \ddot{z} = \frac{-\mu z}{(\rho^2 + z^2)^{3/2}} \tag{3}$$

B.4 Elliptic Coordinates, Set 1

$$\ddot{\alpha}_1 = 0 \qquad \ddot{\alpha}_2 = \frac{-\mu e \sin v}{a^3(1 - e \cos v)^3} \qquad \ddot{\alpha}_3 = 0 \tag{4}$$

B.5 Elliptic Coordinates, Set 2

$$\ddot{\beta}_1 = 0 \qquad \ddot{\beta}_2 = \frac{\mu(e - \cos v)}{a^3(1 - e \cos v)^3} \qquad \ddot{\beta}_3 = 0 \tag{5}$$

BIBLIOGRAPHY

1. Gerber, W. J., Lewallen, J. M., "Numerical Error Comparisons for Integration of Near Earth Orbits in Rectangular and Spherical Coordinates," MSC-IN-66-ED-39, MSC Internal Note, National Aeronautics and Space Administration, Manned Spacecraft Center, August 1966.

2. Rainbolt, Mansell, Lewallen, J. M., (Private communication of unpublished material), National Aeronautics and Space Administration, Manned Spacecraft Center, 1967.

3. Fowler, W. T., Lastman, G. J., "Fortran Subroutines for the Numerical Integration of First Order Ordinary Differential Equations," EMRL RM 1024, The University of Texas, March 1967.

4. Margenau, H., Murphy, G. M., The Mathematics of Physics and Chemistry, D. Van Nostrand Company, Inc., 1943, Pages 172-182.

5. Ehricke, K. A., Space Flight, Volume I, Environment and Celestial Mechanics. D. Van Nostrand Company, Inc., 1959.

6. Nelson, W. C., Loft, E. A., Space Mechanics, Prentice-Hall, Inc. 1962.

7. Morse, P. M., Feshbach, H., Methods of Theoretical Physics, Part I, McGraw-Hill Book Company, Inc., 1953.

8. Spiegel, M. R., Vector Analysis, Schaum Publishing Company, 1959.